Alma Mater Studiorum – Università di Bologna

DOTTORATO DI RICERCA IN

GEOFISICA

Ciclo XXVII

Settore Concorsuale di afferenza: 04 / A4 - Geofisica

Settore Scientifico disciplinare: GEO / 10 - Geofisica della Terra Solida

OBLIQUE IONOGRAMS AUTOMATIC SCALING AND EIKONAL BASED RAY TRACING

Presentata da: Alessandro Ippolito

Coordinatore Dottorato   **Relatore**

Prof. Michele Dragoni   **Dott. Carlo Scotto**

Esame finale anno 2015

Contents

1 The Earth's Ionosphere

The ionised layer of the uppermost portion of Earth's atmosphere, called the ionosphere, is an important subject of study relevant to numerous technological applications involving radio signals, like over-the-horizon radar techniques and the Global Positioning System (GPS). The ionosphere plays a unique role in the terrestrial environment because of its marked coupling with the overlying and underlying regions. The existence of a conductive layer in the upper atmosphere affected by variations in the magnetic field was first postulated by Gauss in 1839 and taken up by Kelvin in 1860. Marconi established the first experimental evidence for the existence of an ionised layer affecting the propagation of electro-magnetic waves in 1901. After his experiment it was clearly necessary to explain how radio waves could travel across the Atlantic ocean. Many physicists of the time simply suggested that a special type of electromagnetic wave that followed the curvature of Earth was involved. However, in 1902 the American engineer A. Kennelly and the British physicist O. Heaviside suggested that an electrically conducting region in the atmosphere could explain Marconi's results. In the 1920s Appleton and Barnet proposed the theory of a reflective conductive region based on their experimental results. In recent decades there have been numerous important studies on ionospheric physics due to the widespread use of the HF radio spectrum for civil and military communications and an increasing use of satellite-Earth communication systems. The most important characteristic of the ionosphere is that it reflects radio waves up to 30 MHz, making it increasingly important to understand the physical processes involved in the formation and variability of the ionospheric layer in the atmosphere and radio wave propagation in this plasma medium. When a HF radio wave encounters the ionosphere it can be reflected, refracted, or absorbed depending on its frequency, on the frequency of the electrons in the plasma, and the refractive index of the medium (Rawer, K., 1963).

1.1 Space Weather and Ionospheric studies

Sun-Earth interactions play the leading role in the formation of the Earth's ionosphere, representing an example of natural plasma creation due to solar photoionization and soft x-ray radiation. The Sun emits energy through flares of electromagnetic radiation and energetic electrically charged particles in coronal mass ejections (CME) and plasma streams. This continuous stream of emissions is called *solarwind*. It travels at over 1.5 million km/hour and carries parts of the Sun's magnetic field toward Earth. As the solar wind approaches it is deflected by the Earth's magnetic field. Monitoring and studying solar activity has became an important field of research since phenomena like solar flares, coronal mass ejections,

and solar energetic particles can affect the terrestrial environment and be harmful for human high-tech systems. All these phenomena are part of what is called *spaceweather*. The use of this term to define a field of studies became common in the 1990s, when it was realized that these forms of solar activity pose a serious threat to the increasingly complex communications and technological systems. Violent solar phenomena produce space weather effects on Earth, disrupting HF radio transmissions, damaging power grids, threatening satellite transmissions and instruments, affecting avionics in extreme circumstances, and reducing the useful life of satellites in low Earth orbits. Even long distance pipelines can be put at risk by reducing the efficiency of anti-corrosion cathode systems. As reliance on technology grows, so does the impact of space weather events.

Radio propagation via ionospheric channels is an important means of long-distance radio communication (Kirby et al, 1934; Yeang C., 2004). Thousands of civil and military operators use the ionosphere every day to maintain contact over vast distances. In order to fully exploit these propagation modes it is crucial to understand the physics behind the "magic". Many ionospheric models have been developed in recent years in order to understand and circumvent ionospheric perturbations related to solar activity. Long term variations in the ionosphere and correlated with solar cycles are well understood (Rawer K., 1963), while short term variations are still the object of study, with real time data analysis providing a description of the ionosphere within certain degrees of reliability. One of these empirical models is the IRI model (Rawer et al., 1978), which is a global model for the electron density profile at a given time, latitude, and longitude. The IRI combined a number of different empirical models integrated with data from worldwide ionosondes and satellites.

However, the physical models are the most reliable, like for example the more complex versions developed in the Global Assimilation of Ionospheric Measurement (GAIM) program. These techniques have been extensively applied in oceanography and meteorology, while their application in space physics has been hindered by a lack of availability of real time data. This highlights the importance of constant monitoring of ionospheric conditions through real time data analysis. One possible approach to better understand the ionosphere is to investigate this layer by oblique ionospheric sounding with automatic interpretation of the resulting oblique ionograms. The latter contain a large quantity of information about the physical parameters of the ionosphere over extended geographical areas, representing the radio-propagation channel between transmitter and receiver.

1.2   The Present Work

This study addresses the issue of understanding the ionospheric medium through analysis of oblique ionospheric soundings. An algorithm is presented for the au-

tomatic interpretation of oblique ionograms, which in turn is proposed as a useful means for monitoring the ionospheric layer, with important applications in space weather observations. Oblique soundings carry information regarding a large region of the ionosphere, thereby offering much more data on the physical parameters compared to vertical ionograms. Computer programs already exist for the automatic interpretation of vertical ionograms (Scotto and Pezzopane, 2002; Gilbert and Smith, 1988), but as yet there are no methods for automatic scaling of oblique ionograms. The results presented below demonstrate how the autoscaling program described in this paper allows real-time evaluation of MUF values for a particular radio link using an oblique radio sounding. The automatic recognition of the "nose" of the ionogram also enables determination of the time taken by the radio wave to travel between the transmitter and receiver at frequencies just below the MUF. The successful reconstruction of an ionogram trace indicates the possibility of estimating electron density between a transmitter and receiver through the analysis of oblique soundings. Using a ray tracing procedure based on the eikonal equation, the ionospheric region along the ray path is modeled.

References

[1] Gilbert, J. D. and Smith, R. W., *A comparison between the automatic ionogram scaling system ARTIST and the standard manual method*, Radio Science, Volume 23, Number 6, Pages 968-974, November-December 1988.

[2] Kirby, S. S., Berkner, L. V. and Stuart, D. M., *STUDIES OF THE IONO-SPHERE AND THEIR APPLICATION TO RADIO TRANSMISSION*, Part of Bureau of Standards Journal of Research, vol. 12, January 1934.

[3] Rawer, K., *Meteorological and Astronomical Influences on Radio Wave Propagation*, Academic Press, New York, 1963.

[4] Rawer, K., Bilitza, D. and Ramakrishnan, S., *Goals and status of the International Reference Ionosphere*, Reviews of Geophysics, Vol. 16, pp. 177181, May 1978.

[5] Scotto, C. and Pezzopane, M., *A Software for Automatic Scaling of foF2 and MUF(3000)F2 from Ionograms*, Proceedings of the XXVII General Assembly of the International Union of Radio Science, 1724, Maastricht, The Netherlands, August 2002.

[6] Yeang, C., *Characterizing Radio Channel: The Science and Technology of Propagation and Interference, 1900-1935*, 2004 .

2 Ionospheric Plasma

As already mentioned, the proportion of free electrons present in the Earth's ionosphere that persist for long enough periods before recombining into neutral atoms or molecules, is sufficient to affect radio wave propagation. This occurs 75 to 1000 km above the Earth and due to ionization from solar and cosmic radiation. The plasma layer of the atmosphere does not simply float above the Earth but is constantly fed from outside. The Earth is continuously bombarded from outer space by various types of radiation. Some of this radiation has such high energy that it can knock electrons out of orbit from gas atoms in the atmosphere, thereby creating ions and free electrons. The number of free electrons per volume unit is referred to as the ionospheric plasma density. Free electrons and ions are generated from the ionization of neutral particles both by extreme ultraviolet radiation from the Sun and by collision with energetic particles that penetrate the atmosphere. Solar radiation at ultraviolet (UV) and shorter wavelengths is classed as "ionizing" since photons of energy at these frequencies are capable of dislodging an electron from a neutral gas atom or molecule upon collision. At these altitudes neutral atmospheric particles within the ionosphere still outnumber free electrons by about 10000 : 1, with the result that the free electrons persist for long periods before recombining. Fundamental differences in the ionization processes that occur in the upper part of Earth's atmosphere, result in a layering of the ionosphere with altitude. Many studies have shown that the number of free electrons per unit volume slowly increases with height within a given layer of the ionosphere, reaching a maximum after which it drops abruptly with further increasing height. The Earth's ionospheric layer is generated by irradiative interaction with the Sun, and so its variations in proprieties are closely related to solar activity, height, longitude, latitude, seasons, day, and time. For example, as shown in the left panel of Figure 1, ionospheric structure varies markedly from day to night because solar photons are the major ionizing factor.

Once formed, the charged particles are affected by a wide range of processes, including chemical reactions, diffusion, wave disturbances, plasma instabilities, and transport due to electric and magnetic fields. Hence, an understanding of ionospheric phenomena requires a knowledge of several disciplines, including plasma physics, chemical kinetics, atomic theory, and fluid mechanics.

2.1 Ionizing Agents

The primary source of plasma and energy for the ionosphere is solar EUV, UV, and Xray radiation (Hargreaves et al., 2007; Frank-Kamenetsky and Troshichev, 2012),

but magnetospheric electric fields and particle precipitation also have a significant effect (Hargreaves, J.K., 2010). It conventional to think of the ionosphere as a number of distinct layers. This is a convenient simplified scheme, but not entirely accurate because the entire ionosphere contains ionized molecules and free electrons. Instead, the layers are best thought of as peaks in ionization levels, as seen in Figure 1. Solar radiation leads to ion-electron production and heating via photo-electron energy degradation, with EUV wavelengths dominating in the lower thermosphere (E and F_1 regions), and UV and X-ray wavelengths dominating in the mesosphere (D region). These processes occur over the entire sunlit side of the Earth. On the night side, resonantly scattered solar radiation and starlight are important sources of ionization for the E region. The production of ionization due to auroral precipitation and the Joule heating that is associated with electric convection fields are maximized in the E and F_1 regions. The F_2 layer is the most important for HF radio wave propagation because it contains the densest plasma of all the atmospheric regions and n_e assumes maximum values of about $10^{(12)}$ $m^{(-3)}$ in this layer.
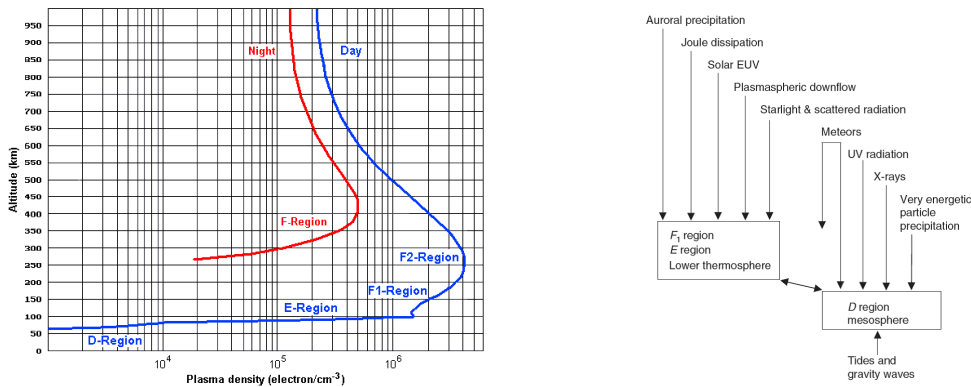
Figure 1: The left panel shows the typical electron density profile in the ionosphere. The right panel shows the external processes that act on the terrestrial ionosphere.

2.2   Electronic Equilibrium

The balance between the varying wavelengths or energies of the electromagnetic and particle radiation producing the ionization means that both the positive and negative ions are too heavy to interact with the oscillations of the electric field carried by the HF radio waves, and so radio wave propagation at these frequencies is almost completely influenced by free electrons, the density of which in the ionosphere varies mainly in altitude. Between 1 and 30 MHz the ionosphere is an essential component for propagation, which is why it is common to consider electron density n_e as the

characteristic parameter of the ionosphere. This value varies from point to point and is the result of many processes such as production, transport, and disappearance of electrons (Aminaei et al., 2006). If we consider a given point in the ionosphere at a given time, the electron density can be described with the equation:

$$\frac{dn_e}{dt} = q - l + d \tag{1}$$

where q is the production rate of electrons, l is the disappearance rate and d is the transport rate.

The different elements that represent the main constituents of the atmosphere at difference altitudes, form the basis for the photochemical processes involving the production or disappearance of free electrons.This is why n_e is not linear with height and electron density reaches its maximum value around 250 km, corresponding to the F_2 region. The Earth's ionosphere is commonly divided into two parts known as the bottomside, the zone underlying the absolute maximum of electron density, and the topside, which is the upper zone of the ionospheric region overlying the absolute maximum of electron density.

Since the nature of the ionosphere is strongly linked to fluctuations in solar emissions, it is highly variable. On short time-scales, solar X-ray radiation can increase dramatically when solar flares occur, increasing D and E region ionization. During geomagnetic storms the auroral source of ionization becomes much more intense and variable, expanding to lower latitudes. The other main source of variability in the ionosphere comes from charged particles responding to the neutral atmosphere in the thermosphere. The ionosphere also responds to thermospheric winds, which can push the ionosphere along the inclined magnetic field lines to a different altitude. During a geomagnetic storm, the energy input at high latitudes produces waves and changes in thermospheric wind composition. Tides and gravity waves effect ionization in the E region and they both cause the concentration of ionization into layers. Depending on the density of the electrons, their range of movement, the frequency and amplitude of the radio waves, the effects can range from total absorption of the radio waves to selective reflection and phase delays (Pillet G., 1960; Stauning P., 1998).

References

[1] Aminaei, A., Honary, F., Kavanagh, A. J., Spanswick, E. and Viljanen, A. , *Characteristics of night-time absorption spike events*, Ann. Geophys., 24, 18871904, 2006

[2] Bailey, D. K., *POLAR-CAP ABSORPTION*, Planet. Space Sci., Vol. 12, pp. 495 to 541. , 1964.

[3] Frank-Kamenetsky, A. and Troshichev, O., *A relationship between the auroral absorption and the magnetic activity in the polar cap*, Journal ofAtmospheric and Solar-Terrestrial Physics, 77, 4045, 2012.

[4] Hargreaves, J.K., *Auroral radio absorption: The prediction question*, Advances in Space Research, 45, 10751092, 2010.

[5] Hargreaves, J. K., Birch, M. J., and Bromage, B. J. I., *D- and E-region effects in the auroral zone during a moderately active 24-h period in July 2005*, Annales Geophysicae, 25, 18371849, 2007.

[6] Pillet, G., *Contribution a l'etude de l'absorption ionospherique sur une frequence fixe*, Annales des Telecommunications, 1960.

[7] Sauer, H. H. and Wilkinson, D. C., *Global mapping of ionospheric HF/VHF radio wave absorption due to solar energetic protons*, SPACE WEATHER, VOL. 6, S12002, doi:10.1029/2008SW000399, 2008.

[8] Stauning, P., *Substorm modeling based on observations of an intense high-latitude absorption surge event*, JOURNAL OF GEOPHYSICAL RESEARCH,VOL. 103, NO. A11, PAGES 26,433-26,452, 1998.

3   HF Propagation in the Ionosphere

When a high frequency radio wave passes through ionospheric plasma, the free electrons respond by moving, generating their own electro-magnetic field. If the transmitted frequency is higher than the plasma frequency, the electrons cannot respond fast enough, and they are not able to generate a new electro-magnetic field, so the transmitted waves can pass right through the ionised layer. However, the free electron density in the ionosphere is a function of height, and so when the frequency of the transmitted radio wave is the same as the plasma frequency of the ionospheric layer, the energy of the wave is absorbed by the electrons, causing them to vibrate at the same frequency. This generates a new electro-magnetic wave in the opposite direction to the original transmission, so that the original transmitted wave appears to be reflected back to the ground by the presence of the free electrons. Since the ionosphere varies on time scales that can be less than a few minutes, information regarding available frequencies needs constant updating. The changing state of the ionosphere is generally monitored by networks of vertical ionosondes, providing real-time information on the state of the ionosphere. An oblique ionospheric sounder extends this idea: the transmitter and receiver of an oblique sounder are not co-located like vertical ones, but are generally hundreds or even thousands of kilometers apart, so the instrument is able to study how the radio signals of real communications propagate via the ionosphere under a variety of conditions. However, the interpretation of oblique propagation is also significantly harder than for vertical sounding. Oblique incidence sounding also provides an excellent test of ionospheric forecasting tools, since ray tracing through the predicted electron density structure can be compared directly to the measured group delays on the oblique path. The propagation of electro-magnetic waves in a medium is described by the Maxwell equations, and the wave behavior is strongly influenced by the spatial distribution of the refractive index of the medium. The theory describing radio wave propagation in uniformly magnetized plasma is known as Magneto-ionic theory (Ratcliffe, J. A., 1959 ; Flood, V. A., 1959). A magneto-ionic medium is a medium comprising free electrons and heavy positive ions in a uniform magnetic field, statistically distributed such as to not present charge separations on macroscopic scales. This condition is satisfied in the Earth's ionosphere, where matter is present in the form of weakly ionized gas and the interaction energy between charged particles is much smaller than their thermal energy. The ionosphere is here considered as a homogeneous magneto-ionic medium which varies with a scale length much smaller than the wavelength considered. The absolute dielectric constant ϵ, magnetic permeability μ and conductivity σ, vary gradually in space.

Under these assumptions and considering the ionosphere as a cold magnetized plasma, the Magneto-ionic theory reconstructs the Appleton-Hartree equation (Sen

and Wyller, 1960; Flood, V. A., 1980) for the phase complex refractive index:

$$n^2 = 1 - \frac{X}{1 - iZ - \frac{Y_T^2}{2(1-X-iZ)} \pm \sqrt{\frac{Y_T^4}{4(1-X-iZ)^2} + Y_L^2}} \tag{2}$$

$Z = \frac{\nu_e}{\omega}$ is the complex term of the equation which takes into account the collisions between electrons and neutral molecules (Budden, K. G., 1965); $Y = \frac{\omega_B}{\omega}$ is the contribution of the Earth's magnetic field, which generates an anisotropy in the medium and consequently the bi-refraction phenomena. This is related to the two different modes of propagation of HF radio waves in the ionosphere, known as ordinary and extraordinary modes. The term $X = \frac{\omega_p^2}{\omega^2}$ describes the relationship between the refractive index and the plasma frequency ω_p, which is a function of the electron density in the ionosphere.

$$\omega_p = \sqrt{\frac{N_e e^2}{\epsilon_o m_e}} \tag{3}$$

The real part of the refraction index can be seen as associated to the wave front propagation of the electro-magnetic wave, while its imaginary part is related to the damping of the wave (Nicolet M., 1953). Ignoring the collisional term, when the phase refractive index is $n_f = 0$, there is no more propagation, which means that this is the required condition for the wave to be reflected by the ionospheric layer. In addition, even when the magnetic field is ignored, the phase refractive index is expressed as:

$$n_f = \frac{c}{v_f} = c\frac{k}{\omega} \tag{4}$$

while the group refraction index is :

$$n_g = \frac{c}{v_g} = c\frac{dk}{d\omega} = \frac{d(ck)}{d\omega} \tag{5}$$

then

$$n_g = \frac{c}{v_g} = \frac{d(\omega \cdot n_f)}{d\omega} = n_f + \omega\frac{dn_f}{d\omega}. \tag{6}$$

As n_f is a function of ω , it can be written as:

$$n_g = \sqrt{1 - \frac{\omega_p^2}{\omega^2}} + \omega\frac{d}{d\omega}\sqrt{1 - \frac{\omega_p^2}{\omega^2}} \tag{7}$$

which, once solved, gives the relationship between the phase refractive index and the group refractive index:

$$n_g = \frac{1}{n_f}. \tag{8}$$

When $n_f \to 0$ then $n_g \to \infty$, as can be seen in equation (5), this implies that $v_g \to 0$. Since v_g is associated with the energy transport of the wave, there is no more transport when n_f reaches 0, and the ray is reflected.

The angle of incidence at which the radio waves enter the ionosphere, defines the path that will be followed by the waves on their way back to Earth. This angle should be small enough for the waves to be reflected back to Earth and large enough so that the waves will not penetrate the ionospheric layer (Sonnenschein et al., 1997). Smaller critical angles should be used for smaller frequencies and larger critical angles for larger frequencies so that they do not penetrate the ionospheric layer and are lost into space.

References

[1] Budden, K. G., *Effect of Electron Collisions on the Formulas of Magneto-Ionic Theory*, RADIO SCIENCE Journal of Research NBSjUSNC- URSI Vol. 690, No.2, February 1965.

[2] Flood, V. A., *A D region mid-and high-latitude approximatioton the Sen-Wyller refractive index equations*, Radio Science, Volume 15, Number 4, pages 797-799, July-August 1980.

[3] Flood, V. A., *The magneto-ionic theory and its applications to the ionosphere*, University Press, 1959.

[4] Nicolet, M., *The collision frequency of electrons in the ionosphere*, Journal of Atmospheric and Terrestrial Physics, vol. 3,pp. 200-211, 1953.

[5] Sen, H. K. and Wyller, A. A., *On the Generalization of the Appleton-Hartree Magnetoionic Formulas*, JOURNAL OF GEOPHYSICAL RESEARCH,vol. 65, No. 12, 1960.

[6] Sonnenschein, E., Censor, D., Rutkevich, I. and Bennett, J. A., *Ray trajectories in an absorbing ionosphere*, Journal of Atmospheric and Solar-Terrestrial Physycs, vol. 59, No. 16, pp. 2101-21 IO, 1997.

4 Ionospheric Monitoring with HF Techniques

Since ionospheric plasma frequency values are typically comparable with HF radio frequencies, it appears useful to use electromagnetic waves in the HF range to study the ionospheric layer of the Earth. The most widely applied technique to study the ionosphere is by vertical ionospheric sounding using a variable frequency radar called an ionosonde. This consists of a high frequency transmitter, a HF receiver, and an antenna with a suitable radiation pattern. In vertical sounding the transmitter automatically emits a radio signal at different high frequencies, typically from 1 to 30 MHz. The receiver measures the time delays between the initial transmission and reception of the reflected signals. Plotting time delays against frequencies gives what is known as a vertical ionogram. An oblique ionogram is obtained from a similar technique to vertical sounding, but with the TX and RX separated, again recording the time delays at different frequencies. Oblique sounding can be very interesting and useful for studying ionospheric regions above geographic locations where it is impractical to build vertical ionosondes, like marine areas.
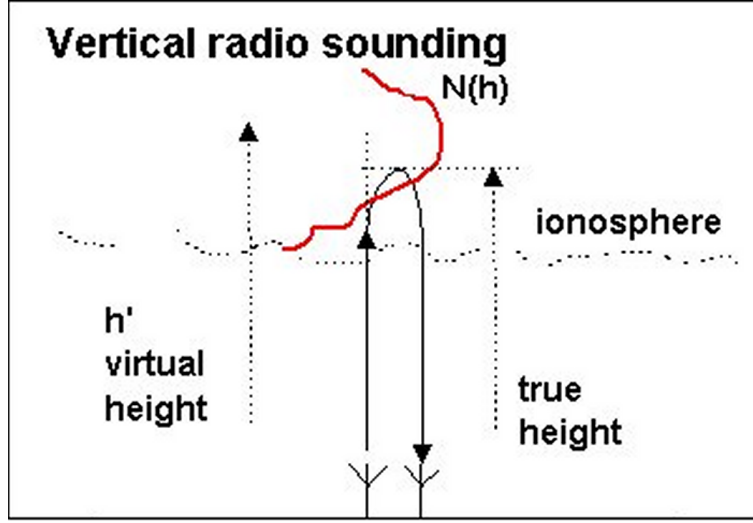
4.1 Vertical Ionospheric Sounding Technique

The presence of several layers of plasma, with densities and relative positions varying with height, makes the reflection of HF radio waves off the ionosphere highly complicated (Bowman and Monro, 1988; Bowman et al., 1988). Most ionospheric research is thus focused on understanding the variations in electron density relative to vertical height above the Earth's surface (Gethinq, 1969) Vertical sounding with a vertical ionosonde involves measuring the time interval of reflection of a radio wave from the ionosphere. Reflection is caused by free electrons present in this region. A computer program measures the time delay Δt for each emitted frequency and the virtual height of reflection is then calculated using the relationship:

$$h' = \frac{c\Delta t}{2} \tag{9}$$

As shown in Figure 2, the virtual high represents the altitude where the electromagnetic wave would be reflected if its velocity was the speed of light c .

4.2 Oblique Ionospheric Sounding Technique

Unlike vertical sounding, in oblique sounding the transmitter and receiver are not co-located but are generally thousands of kilometers apart. The instrument is able to assess how radio signals of real communications, below 30 MHz, propagate via

Figure 2: Scheme of vertical ionospheric sounding in which a transmitter emits a radio wave at HF frequency which, after being reflected by the ionosophere, is detected at ground level by a receiver (Rutherford Appleton Laboratory, 2000).

ionospheric channels under a variety of conditions. However, the interpretation of oblique propagation is also significantly more difficult than for vertical propagation. Figure 3 shows a schematic radio link between a transmitter T and a receiver R, at distance D from T. A HF radio wave emitted from T at a certain elevation angle α, is reflected by the ionosphere at point P at height h above the ground. The electro-magnetic wave in the HF range of frequencies, called sky wave, is not actually reflected, but is refracted along its entire path. Considering a uniformly stratified ionosphere, its direction changes continuously as it goes through the ionospheric layers, following Snell's law:

$$\frac{n_1}{n_2} = \frac{\sin \theta_r}{\sin \theta_i} \tag{10}$$

So the ray path is curved because the phase refractive index n_f decreases with altitude, as the electron density $N_e(h)$ increases.

After each refraction, the radio wave path is much closer to the horizontal interface between the layers characterized by different refractive indexes, until the critical angle of incidence is reached:

$$\theta_c = arcsin \frac{n_{i_{max}}}{n_{i_{max-1}}} \tag{11}$$

with the limit condition:

15
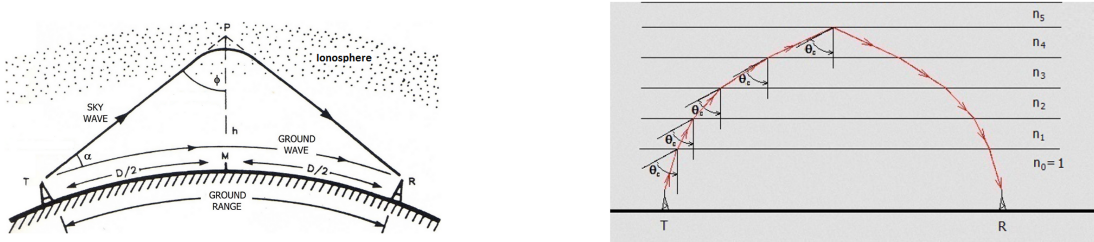
Figure 3: The left panel shows a schematic oblique ionospheric sounding. Unlike vertical soundings, the transmitter and receiver are separated. The right panel shows the refraction of the radio wave through the ionosphere due to the different refraction indexes of the ionospheric layers.

$$\theta_c^{lim} = \frac{\pi}{2} \tag{12}$$

after which the electro-magnetic wave will begin its return path to the ground. Once detected by the receiver, the group delay is measured for the particular radio frequency. Varying the carrier frequency of the pulses, typically from 2 to 30 MHz, is produced an oblique ionogram, usually presented in the form of a graph in which the time delay is plotted against frequency as in vertical ionograms.

4.3 Ionospheric Parameters Deduced by Ionograms Interpretation

Many important physical parameters of the ionospheric regions intersected by radio soundings can be deduced from interpretation of vertical and oblique ionograms, making these the most important techniques for studying the physics of the ionosphere. As shown in Figure 4, vertical ionograms can provide important ionospheric parameters, such as the critical frequencies of the different ionospheric layers (Hargreaves and Friedrich, 2003; Hargreaves et al., 2007), the respective virtual heights, and the electron density distribution in the region above the vertical ionosonde. The maximum frequency reflected vertically by the ionospheric F_2 layer at a given time and place is known as $f_0 F_2$. The extraordinary mode reflecting off the F_2 layer is known as $f_x F_2$. Similarly, the maximum frequencies reflected by the E layer and F_1 layer are known as $f_o E$ and $f_o F_1$, respectively. All the virtual heights as a function of the different vertical sounding frequencies, are plotted in the vertical ionogram (Figure 4). The anisotropy introduced by the Earth's magnetic field is the reason for the bi-refraction phenomena producing the two different traces on the ionogram. The red trace, in the example of Figure 3, represents the ordinary mode of propagation of the radio wave, while the green trace is the extraordinary mode. Unlike
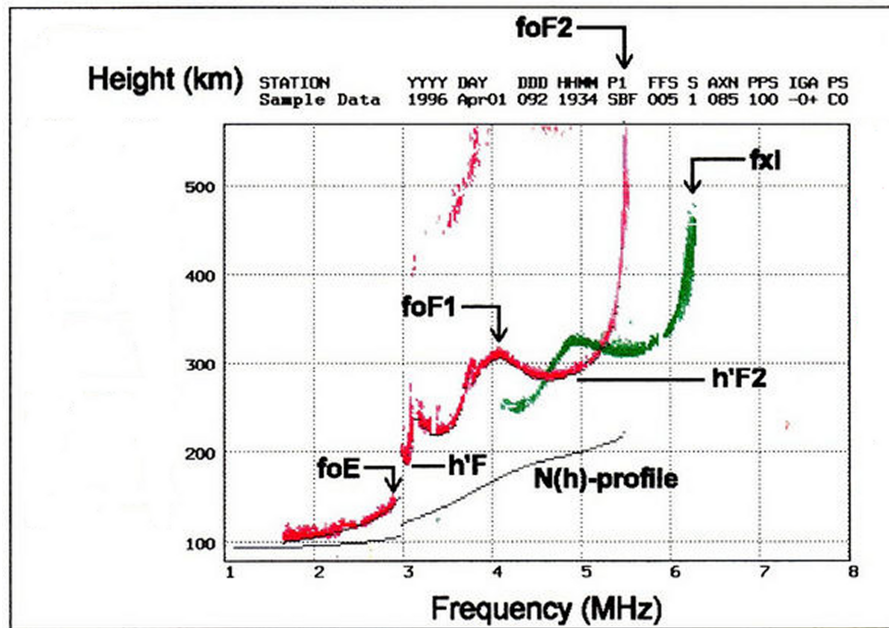
Figure 4: Example of vertical ionogram (Reinisch, B. W., 2003). The two different traces are due to the bi-refraction generated by the Earth's magnetic field. Numerous important physical ionospheric parameters can be deduced from a vertical ionogram.

vertical soundings, oblique soundings have the advantage of detecting ionospheric parameters over wider regions, where it might not be practical to deploy vertical sounders, like for example marine areas and other difficult terrain. Oblique ionosondes also provide more ionograms with less transmitting and receiving devices. The interpretation and study of oblique ionograms gives a lot of valuable information on the ionospheric region between the transmitter and receiver.

Oblique ionograms provide high-resolution images that permit quick identification of the frequencies that are propagating between given transmitter and receiver stations. They also reveal the available communication bands and any gaps where no links can be established. These features of a channel are very important because the information on available frequencies needs to be constantly updated, considering that the ionosphere changes on a time scale of few minutes. As with vertical sounding, oblique sounding also presents the peculiarity of two different traces. Once again this derives from the anisotropy introduced by the Earth's magnetic field, which produces two different paths for the same frequency, depending on the polarization of the electro-magnetic wave. The most significant value that can be measured from an oblique ionogram is known as MUF, or Maximum Usable Frequency, which defines the highest usable frequency for a particular radio link. It refers to the frequency

of the "nose" of the ordinary trace of the oblique ionogram, as shown in Figure 5. Oblique ionospheric sounding also offers several important advantages over vertical
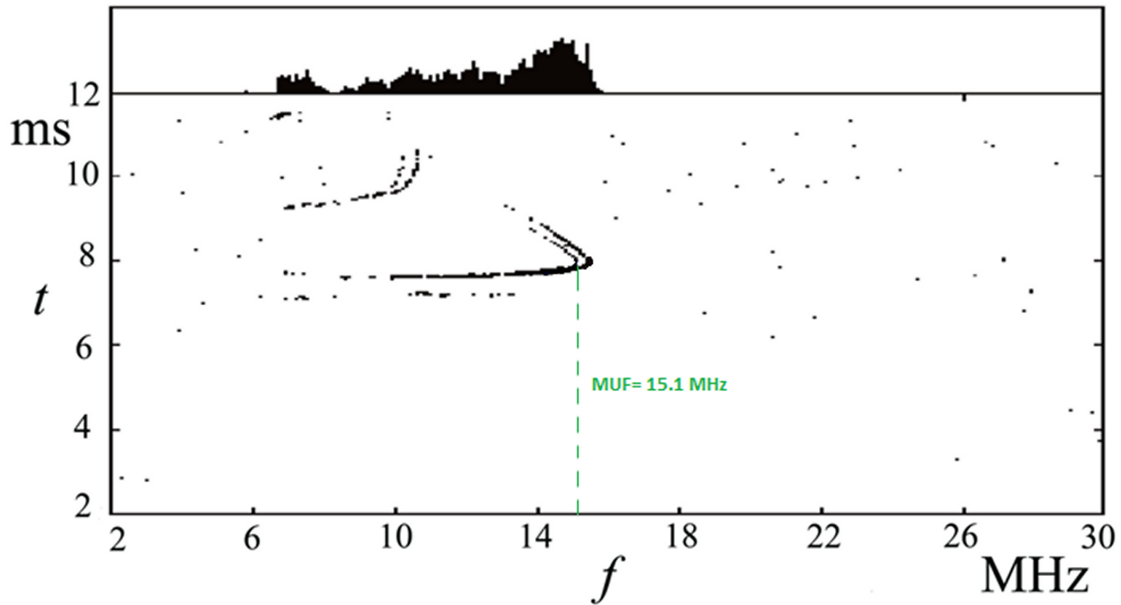
Figure 5: Example of oblique ionogram. The two different traces are due to the bi-refraction induced by the Earth's magnetic field. The MUF (Maximum Usable Frequency) is the frequency corresponding to the "nose" of the ordinary trace.

sounding for the understanding of radio wave propagation and physical parameters of the ionosphere. For example, the possibility of monitoring the ionosphere across large otherwise inaccessible areas like oceans. An obliquely propagating radio wave is refracted and not simply reflected and is much more susceptible to the effects of horizontal gradients and variations in the ionosphere. The situation is further complicated by the fact that radio signals from a transmitter can take a variety of different routes to reach the receiver, adding to the possible sources of signal distortion and loss.

The purpose of an oblique sounding is largely an attempt to understand the factors effecting propagation which will ultimately limit link reliability due to natural ionospheric variability. The variable state of the ionosphere is generally monitored by networks of vertical ionosondes, providing real-time data. Oblique ionospheric sounders, as already explained, extend this concept: the transmitter and receiver of an oblique sounder are not co-located, unlike vertical sounders, and are generally several hundreds or thousands of kilometers apart, so that the instrumentation is

able to study how HF radio signals propagate via the ionosphere under a variety of conditions (Chen et al., 1992).

There are well-established techniques for vertical ionograms making it possible to define the main physical parameters of the ionosphere in real-time. These include the ARTIST system (Reinisch and Huang, 1983; Gilbert and Smith, 1988; Galkin et al. 2008) developed at the University of Lowell, Center for Atmospheric Research, and the Autoscala program from the Italian Istituto Nazionale di Geofisica e Vulcanologia (INGV) (Scotto and Pezzopane, 2002; Pezzopane and Scotto, 2007; Scotto 2009). The data produced by these computer programs can be effectively integrated into real-time and short term forecasting models (Galkin et al. 2012). However, the interpretation of oblique ionograms is significantly more complex, and there are no well established automatic techniques. The reason for the lack of such techniques is partly due to the relative rarity of this type of sounding, at least on a systematic level, so that less effort has been dedicated to them. It is certainly also due to the greater difficulties that these ionograms pose compared to vertical soundings. On the other hand, the information obtained from an oblique HF sounder is much more articulated than that derived from traditional vertical ionogram readings. Noteworthy in this respect are the attempts of Huang and Reinisch (1996) to develop a computationally efficient technique for the inversion of oblique ionograms, in order to obtain mid-point electron density profiles.

Since the inversion of an oblique ionogram is much more difficult than the inversion of a vertical one, poses significant problems on the reconstruction of the ray path (Norman and Cannon, 1999), even because the situation is further complicated by the fact the variety of different paths that radio signals can take, adding possible sources of signal distortion and loss. In the absence, until now, of software for automatic interpretation, oblique soundings have largely been used to try and understand the factors aggravating propagation in order to improve radio link reliability in the face of natural ionospheric variability.

As explained, oblique ionograms contain much more information on ionospheric parameters than vertical ionograms, and this is why, despite being more complex and difficult than vertical ionograms, it is reasonable to assume it is possible to determine the ionospheric structure of the region object of the radio sounding from an oblique sounding. This paper presents an autoscaling algorithm for oblique ionograms. The radio link between Rome (Italy) and Kania (Greece) was considered, using data recorded by INGV. The problem of automatic scaling of oblique ionogram traces is approached using the maximum contrast method, as applied in the Autoscala computer program (Scotto and Pezzopane, 2002), and introducing a new set of empirical curves. The electron density distribution along the path is estimated by a ray tracing procedure based on the eikonal equation (Born and Wolf, 1993).

References

[1] Bowman, G. G. and Monro, P. E. , *Mid-latitude range spread and travelling ionospheric disturbances*, Journal of Atmospheric and Terrestrial Physics, Vol 50, No. 3. pp. 215-223, 1988.

[2] Bowman, G. G., Clarke, R. H. and Meeha, D. H., *Mid-latitude frequency spread and its association with small scale ionospheric stratifications*, Journal of Atmospheric and Terrestrial Physics, Vol. 50, No. 9, pp. 797-809, 1988.

[3] Chen, J., Bennett, J. A., and Dysoni, P. L., *Synthesis of oblique ionograms from vertical ionograms using quasi-parabolic segment models of the ionosphere*, Journal of Atmospheric and Terrestrial Physics, Vol. 54. No. 3/4. pp. 323-331, 1992.

[4] Galkin, I. A., Reinisch, B. W., Huang, X. and Bilitza, D., *Assimilation of GIRO data into a real-time IRI*, Radio Science, VOL. 47, RS0L07, doi:10.1029/2011RS004952, 2012.

[5] Galkin, I. A.,Khmyrov, G. M., Kozlov, A. V., Reinisch,B. W., Huang, X., and Paznukhov ,V. V., *The ARTIST 5, in Radio Sounding and Plasma Physics*, AIP Conf. Proc., 974, 150159, 2008.

[6] Gilbert, J. D. and Smith, R. W., *A comparison between the automatic ionogram scaling system ARTIST and the standard manual method*, Radio Science, Volume 23, Number 6, Pages 968-974, November-December 1988.

[7] Gethinq, P. J. D., *The calculation of electron density profiles from oblique ionograms*, Journal of Atmospheric and Terrestrial Physics, vol. 31, pp. 347-354, 1969.

[8] Gethinq, P. J. D., *Automatic scaling of critical frequency foF2 and MUF(3000)F2: a comparison between Autoscala and ARTIST 4.5 on Rome data*, Journal of Atmospheric and Terrestrial Physics, vol. 31, pp. 347-354, 1969.

[9] Gethinq, P. J. D., *Vertical electron density profiles from the digisonde network*, Advances in Space Research, 18, pp. 121129, 1996.

[10] Hargreaves, J. K., Birch, M. J., and Bromage, B. J. I., *D- and E-region effects in the auroral zone during a moderately active 24-h period in July 2005*, Annales Geophysicae, 25, 18371849, 2007.

[11] Norman, R. J. and Cannon, O. S., *An evaluation of a new two-dimensional analytic ionospheric ray-tracing technique: Segmented method for analytic ray tracing (SMART)*, Radio Science, vol. 34, Issue 2, pp. 489499, 1999.

[12] Reinisch, B. W., *HF RADIO SOUNDING OF GEOSPACE PLASMAS*, 8th International Congress of the Brazilian Geophysical Society, 2003 .

[13] Reinisch, B. W. and Huang, X., *Automatic calculation of electron density profiles from digital ionograms, 3, Processing of bottomside ionograms*, Radio Science, 18 , pp. 477492, 1983 .

[14] Scotto, C., *Electron density profile calculation technique for Autoscala ionogram analysis*, Advances in Space Research, 44, pp. 756766, 2009.

[15] Scotto, C. and Pezzopane, M., *A Software for Automatic Scaling of foF2 and MUF(3000)F2 from Ionograms*, Proceedings of the XXVII General Assembly of the International Union of Radio Science, 1724, Maastricht, The Netherlands, August 2002.

5 Automatic Interpretation of Oblique Ionograms

Although manual scaling is still considered the most reliable technique for ionogram interpretation, automatic scaling represents the only technique that meets modern requirements of ionospheric monitoring for space weather purposes (Wright and Conkright, 2002; Ding et al., 2007; Galkin et al., 2006). The reliability of automatic ionogram interpretation has been discussed from many perspectives (Gilbert and Smith, 1988) and, considering the wider range of data that can be analyzed, automatic scaling is recognized as a very useful scientific tool (Uemoto et al., 2009; Galkin et al., 2012; Stankov et al., 2012). An algorithm has been devised for the identification of trace characteristics of oblique ionograms, allowing determination of the Maximum Usable Frequency (MUF) for communication between the transmitter and receiver. The greater complexity of oblique compared to vertical ionograms is matched by greater information content, providing enormous potential for this technique, which has not yet been fully exploited. It is perfectly reasonable to presume that ionospheric structure can be determined from oblique ionograms, albeit with much more difficulty than from vertical ionograms.

Oblique soundings are significantly affected by absorption phenomena (Lastovicka, J., 1978; Pendorf, F., 1962; Tsunoda, R. T., 2008) especially during solar flare events and polar cap absorption events (PCA) at polar latitudes (MacDougall et al., 1962; Herman J. R., 1966; King G. A. M., 1970). In many cases the typical oblique ionogram traces can completely disappear during these phenomena (Frank-Kamenetsky and Troshichev, 2012; Scotto and Pezzopane, 2011). A test was performed on the algorithm using data from a campaign of oblique soundings between Rome, Italy ($41.90N$, $12.48E$) and Chania, Greece ($35.51N$, $24.01E$), as reported in Figure 6. The transmitting system is based on a VOS-1 chirp ionosonde produced by the Barry Research Corporation, Palo Alto, CA, USA [Barry Research Corporation, 1975] sweeping from 2 to 30 MHz at 100 kHz/s with an average power of less than 10 W (Zuccheretti et al., 2003). The transmitting antenna is a delta for decametric wavelengths used for vertical soundings but also suitable for oblique soundings. The receiver is an RCS-5B chirp produced by the Barry Research Corporation [1989]. The oblique ionograms related to this ray-path are recorded in ".OS2" files, with the group delay for each frequency from 2 to 30 MHz. The files are initially recorded in a special format readable by a dot-matrix printer.

5.1 The Autoscaling Algorithm

The procedure for the reconstruction of oblique ionogram traces is based on the image recognition technique used in the Autoscala program (Scotto and Pezzopane,
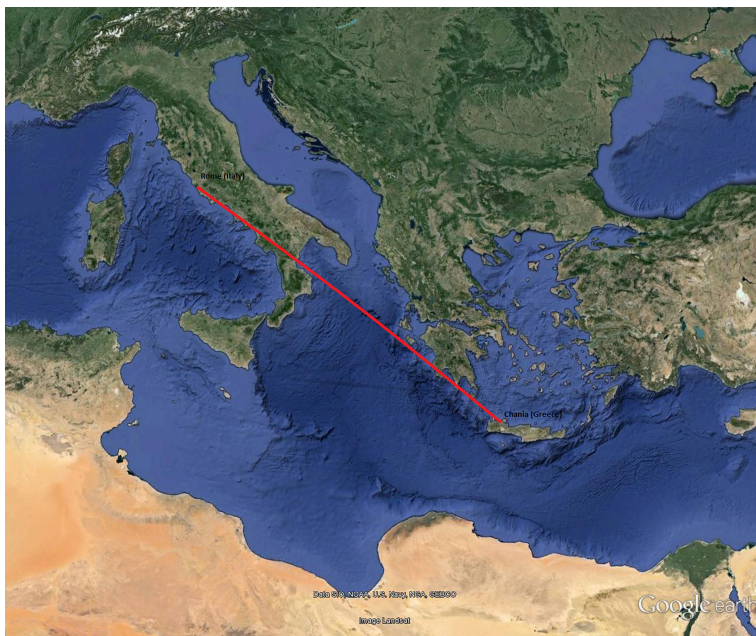
Figure 6: The figure shows the radio link between the ionosondes of Rome, Italy ($41.90N$,$12.48E$) and Chania, Greece ($35.51N$,$24.01E$).

2002) for automatic scaling of both the ordinary and extraordinary traces of a vertical ionogram. The software developed in this work was written in the Visual Basic 6 language. It first adapts each file format to a computer terminal reading, then stores the ionogram as a matrix A, with m rows and n columns, as defined by the following formulas:

$$m = int\left[\frac{(t_f - t_0)}{\Delta t}\right] + 1 \tag{13}$$

$$n = int\left[\frac{(f_f - f_0)}{\Delta f}\right] + 1 \tag{14}$$

where f_f, f_0, Δf , t_f, t_0, Δt, , are respectively the final frequency, the initial frequency, the frequency step, the final time delay, the initial time delay, and the time delay resolution of the oblique sounding. In general, t_0, Δt are fixed values, which depend on the design of the ionosonde. The element a_{ij} (with $i = 1, ..., m$ and

$j = 1, ..., n$) of the matrix A is an integer ranging from 0 to 255 proportional to the amplitude of the received echo. This value being obtained directly from the binary file recorded by the instrument. Once the frequencies and related time delays have been recorded from the input file, the program prints the ionogram (Figure 7).
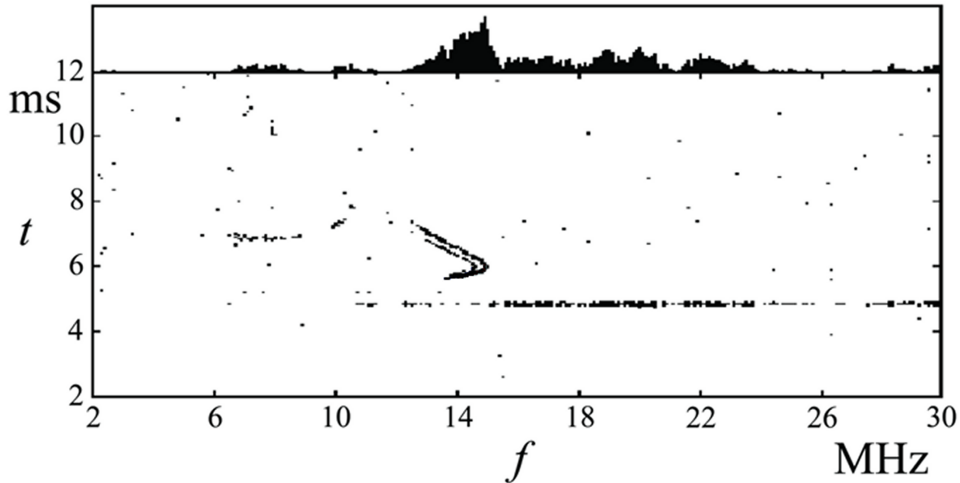
Figure 7: An oblique ionogram recorded on the Rome-Chania radio link on June 25, 2011, at 10:00.

The image recognition technique applied is based on the maximum contrast method: the correlation is calculated between a family of functions defining the typical shape of the ionogram, and the elements of the matrix that describe the ionogram. The analytical curves characterized by the maximum contrast value are recognized as a good model for the ionogram traces. In order to find the family of curves that best fits oblique ionograms, numerous different analytic functions were considered. A number of oblique soundings were analyzed using a cluster of parabolas as an analytical model to identify the oblique ionogram traces and to determine the MUF value. In the example in Figure 8 is shown a test made using a cluster of parabolic branches. In many cases the curves did not cluster around the nose of the traces and so they did not offer a good fit for the ionogram traces. A couple of branches of parabola were then used as correlation functions to fit the typical shape of oblique ionograms. Each couple joins at a vertex which should parameterize the nose of the ordinary and extraordinary trace. After analyzing a data set of more than 200 oblique ionograms, it was noticed that the upper branches of the parabola often did not correctly fit the upper part of the ionogram traces and introduced a considerable

24
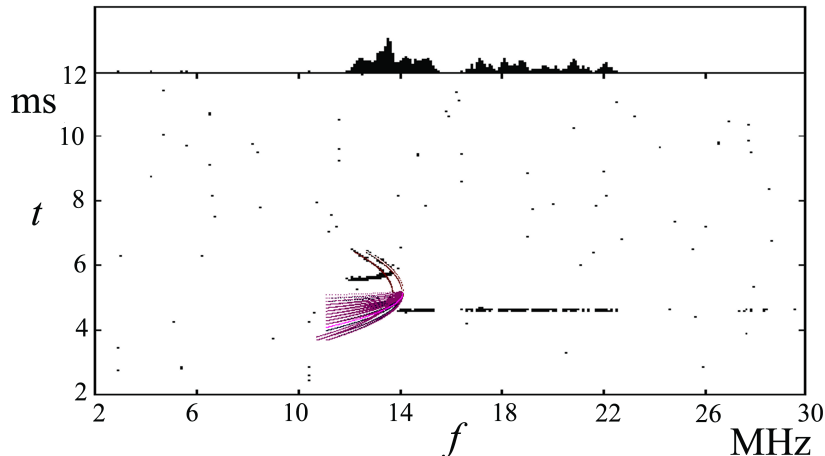
Figure 8: An oblique ionogram recorded on the Rome-Chania radio link on June 25, 2011, at 10:00 and autoscaled using a cluster of branches of parabola.

delay in computation time. Since the most important value that can be deduced from an oblique ionogram is the MUF, which is the vertex of the nose of the ordinary trace, only the two lower branches of the parabolas were used to reconstruct the MUF value of the oblique sounding, minimizing computational time. In this way the algorithm can be useful as a now-casting method for automatic interpretation of oblique ionograms.

Once the ionogram is stored in the form of a matrix of elements a_{ij}, the two empirical curves S_{ord} and S_{ext} are defined. These two curves are able to fit the typical shapes of the ordinary and extraordinary oblique ionogram traces resulting from a single reflection in the F_2 region. The program then calculates the local contrast C between the branch of parabola S_{ord} and the ordinary trace, as well as the contrast between the branch S_{ext} and the extraordinary trace, making allowances for both the number of matched points and their amplitude. The curve S_{ord}, which is used to investigate the ordinary trace, is:

$$t_{ord} = int \left[A_{ord} * f^2 + B_{ord} * f + C_{ord} \right] \tag{15}$$

where f varies within the limits: $f_{v-ord} - \delta f_{ord} \leq f \leq f_{v-ord}$.
The coefficients A_{ord}, B_{ord}, and C_{ord} are related to f_{v-ord}, δf_{v-ord}, t_{v-ord}, δt_{v-ord} in the following relationships:

25

$$A_{ord} = -\frac{\delta f_{ord} - f_{v-ord}}{\delta t_{ord}^2} - \frac{f_{v-ord}}{\delta t_{ord}^2} \tag{16}$$

$$B_{ord} = \frac{2 * (\delta f_{ord} - f_{v-ord}) * t_{v-ord}}{\delta t_{ord}^2} + \frac{2 * (f_{v-ord} * t_{v-ord})}{\delta t_{ord}^2} \tag{17}$$

$$C_{ord} = -\frac{(\delta f_{ord} - f_{v-ord}) * t_{v-ord}^2}{\delta t_{ord}^2} + \frac{f_{v-ord} * (\delta t_{ord}^2 - t_{v-ord})}{\delta t_{ord}^2} \tag{18}$$

Similarly, for the curve S_{ext} used to investigate the extraordinary ray:

$$t_{ext} = int \left[A_{ext} * f^2 + B_{ext} * f + C_{ext} \right] \tag{19}$$

where f varies within the limits: $f_{v-ext} - \delta f_{ext} \leq f \leq f_{v-ext}$.
The coefficients A_{ext}, B_{ext}, and C_{ext} are related to f_{v-ext}, δf_{v-ext}, t_{v-ext}, δt_{v-ext} in the following relationships:

$$A_{ext} = -\frac{\delta f_{ext} - f_{v-ext}}{\delta t_{ext}^2} - \frac{f_{v-ext}}{\delta t_{ext}^2} \tag{20}$$

$$B_{ext} = \frac{2 * (\delta f_{ext} - f_{v-ext}) * t_{v-ext}}{\delta t_{ext}^2} + \frac{2 * (f_{v-ext} * t_{v-ext})}{\delta t_{ext}^2} \tag{21}$$

$$C_{ext} = -\frac{(\delta f_{ext} - f_{v-ext}) * t_{v-ext}^2}{\delta t_{ext}^2} + \frac{f_{v-ext} * (\delta t_{ext}^2 - t_{v-ext})}{\delta t_{ext}^2} \tag{22}$$

The frequencies and time delays of S_{ord} and S_{ext} are expressed as integers and

correspond to the indices i and j of the matrix A. The parameters defining the two curves are:

$$f_{v-ord}, \delta f_{ord}, t_{v-ord}, \delta t_{ord}, f_{v-ext}, \delta f_{ext}, t_{v-ext}, \delta t_{ext}$$

Two integers f_{v-ord} , and t_{v-ord}, are the vertex coordinates in pixels of S_{ord}. Two integers δt_{ord} and δt_{ext}, which vary from 3 to 60, correspond to the width values for both S_{ord} and S_{ext} expressed in pixels, along the t axis. The integers δf_{ord} and δf_{ext} , fixed at 30, represent the extensions in pixels along the f axis of the two branches of the parabola. The abscissa vertex coordinates in pixels of S_{ext}, f_{v-ext}, is linked to f_{v-ord} through the relationship $f_{v-ext} = f_{v-ord} + \Delta f_{ord-ext}$. $\Delta f_{ord-ext}$ corresponds to a frequency of about 0.6 MHz, expressed in pixels. The ordinate vertex coordinates in pixels of S_{ext} varies from t_{v-ord} to $(t_{v-ord}+20)$. The S_{ord} curve (and consequently S_{ext}) is slid across the entire ionogram, and so f_{v-ord} varies from δf_{ord} to $n - \Delta f_{ord-ext}$, while t_{v-ord} varies from δt_{ord} to m. Furthermore, varying the parameters, and thus causing S_{ord} and S_{ext} to change shape while maintaining consistency with the typical oblique ionogram traces shape, results in the vertices moving throughout the ionogram. In this way, for each pair of curves, the local correlation

$$C(f_{v-ord}, \delta f_{ord}, t_{v-ord}, \delta t_{ord}, f_{v-ext}, \delta f_{ext}, t_{v-ext}, \delta t_{ext})$$

with the ionogram recorded, is calculated. In practice, C is the value of the contrast between the pair of empirical curves used to represent the ordinary and extraordinary traces, calculated using the same techniques applied in the electronic processing of the images. The pair of curves S_{ord} and S_{ext} with the maximum C value, called C_{max}, is then selected as shown in Figure 9. The Maximum Usable Frequency (MUF) resulting from a specific oblique sounding can then be inferred from the point V_{ord} of coordinates $(f_{v-ord}; t_{v-ord})$. In automatic scaling procedures the most critical issue is posed by false positive events. These are errors in the data generated by the automatic operation of the program which, in this case, involve an ionogram for which an operator is unable to provide the MUF value, but which is not discarded by the software. The maximum contrast method also provides a criterion for discarding ionograms that do not have sufficient information, in order to avoid false positive events which generate incorrect information about the structure of the ionosphere between the transmitter and receiver. In the algorithm for the automatic scaling of oblique ionograms, only if C_{max} is larger than a fixed threshold C_t, the resulting curves are considered representative of the trace due to reflection from the F_2 region. Otherwise, the ionogram is considered to lack sufficient information and is discarded (Figure 10). In this case, no MUF value is provided as output. Furthermore, it is important to note that the algorithm does not discard ionograms that have a well
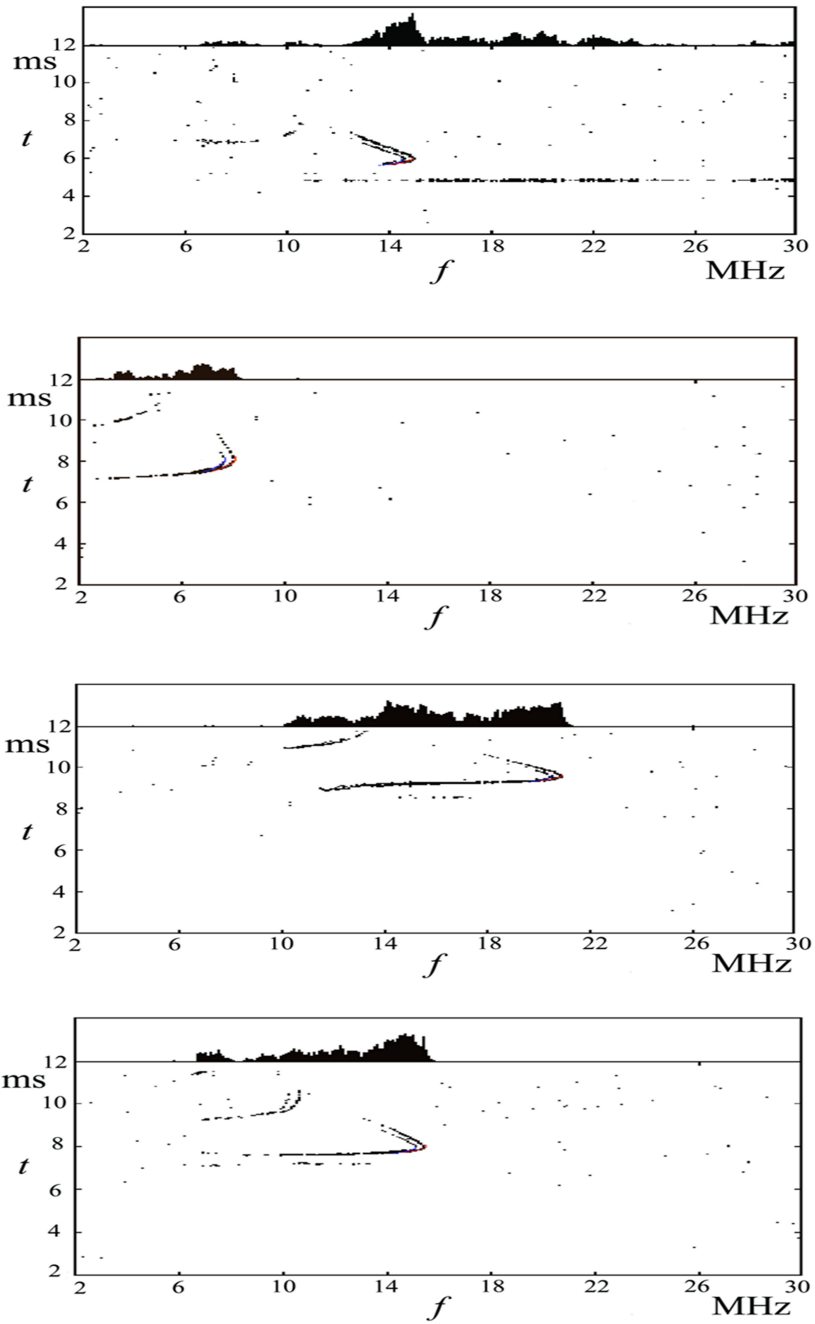
Figure 9: Examples of autoscaled ionograms: ionograms for which both the operator and the software were able to provide the MUF value. The blue and red traces are the two analytic curves with C_{max}, which best fit the oblique ionogram traces.

28

defined traces, from the point of view of an operator, as shown in the examples of Figure 9.

In any case, the presence in the analyzed database of a high percentage of low quality ionograms, makes it possible to efficiently assess the rejection capabilities of the program. The rejection of low quality ionograms represents a major problem in space weather applications. It has been demonstrated that the integration of erroneous data into models has negative effects on the reliability of now-casting and short-term forecasting models, and it is considered preferable to discard questionable data (Galkin, 2012).

5.2 A Preliminary Test of the Autoscaling Program

In order to assess the data errors generated by the automatic operation of the program, the program results were compared with data generated manually by an experienced operator. 272 oblique ionograms were automatically scaled and classified into two groups: subset Y containing ionograms successfully scaled by the software, and subset N containing ionograms considered by the software to lack sufficient information, according to the criteria discussed above.

The subsets were then assessed for:

a) The number of ionograms for which an operator was able to determine the MUF;
b) The number of ionograms for which an operator was unable to determine the MUF.

A quantitative comparison was also performed between the manually scaled values and the corresponding automatically scaled values. This analysis was limited to cases in which both the operator and the software were able to scale the ionogram. In this study, values generated by the software were considered accurate if within 0.5 MHz of the values provided by an operator, while values were considered acceptable if within 2.5 MHz. These limits were chosen in line with the International Union of Radio Science (URSI) standard (Piggott and Rawer, 1972).

These procedures were applied to a data set of 272 ionograms, using five different C_t. This also made it possible to evaluate an appropriate C_t value setting. Table 1 reports a comparison between ionogram figures scaled by an operator and those automatically scaled by the program. It can be seen that for higher C_t values, the number of false positive events is lower.

Table 2 shows the accuracy of automatic scaling for using different C_t. It is clear that the best results are obtained for $C_t = 225$ (Table 1(d)), with the best result in terms of percentage of accurate autoscaled ionograms versus false positive events.
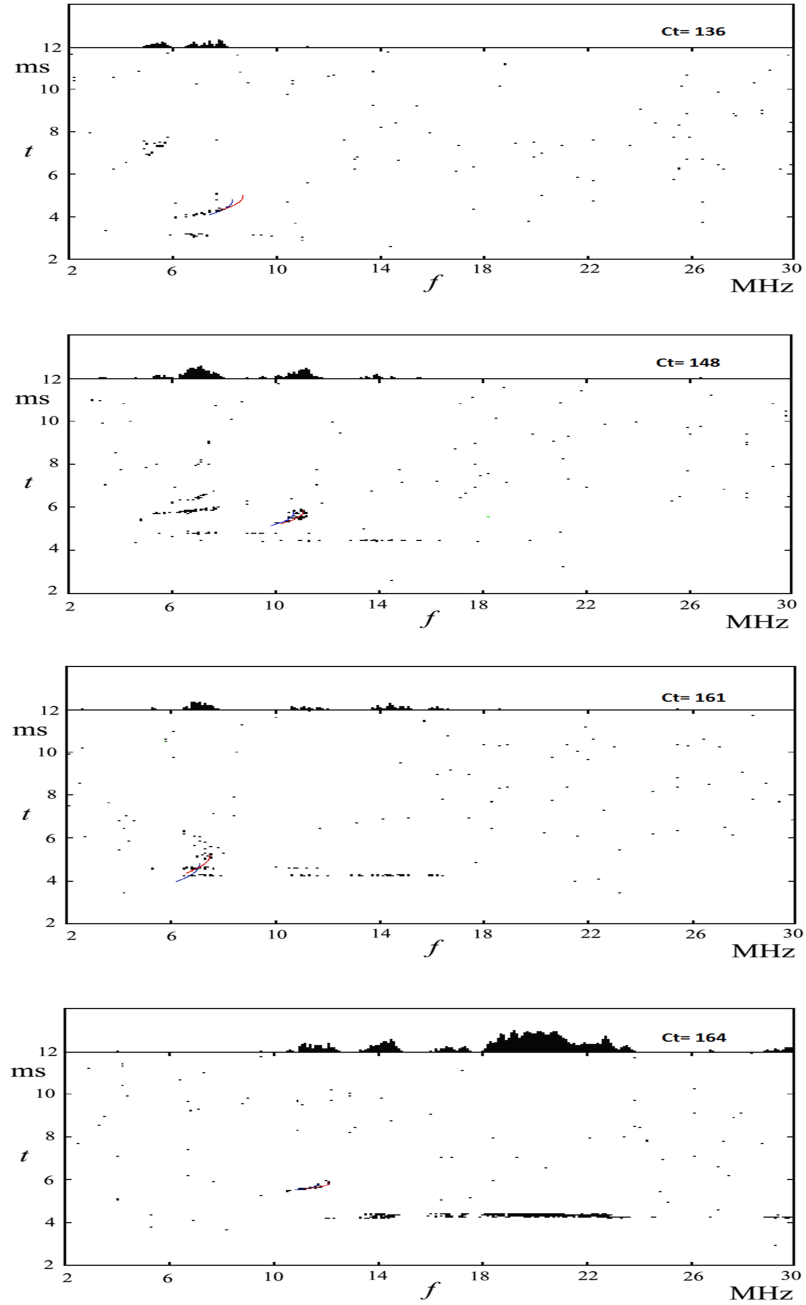
Figure 10: Lack of data ionograms: Ionograms for which C_{max} is lower than the fixed threshold $C_t = 225$. In this case the ionogram is discarded by the software and no MUF value is provided as output.

30

(a)

$C_t = 150$	scaled by the software		discarded by the software	
	No. of cases	%	No. of cases	%
The operator did not scale the MUF	90	52.6	83	82.1
The operator scaled the MUF	81	47.4	18	17.9
Total	171		101	

(b)

$C_t = 175$	scaled by the software		discarded by the software	
	No. of cases	%	No. of cases	%
The operator did not scale the MUF	45	40.2	128	80.0
The operator scaled the MUF	67	59.8	32	20.0
Total	112		160	

(c)

$C_t = 200$	scaled by the software		discarded by the software	
	No. of cases	%	No. of cases	%
The operator did not scale the MUF	14	20.3	159	78.3
The operator scaled the MUF	55	79.7	44	21.7
Total	69		203	

(d)

$C_t = 225$	scaled by the software		discarded by the software	
	No. of cases	%	No. of cases	%
The operator did not scale the MUF	4	10.3	169	72.5
The operator scaled the MUF	35	89.7	64	27.5
Total	39		233	

(e)

$C_t = 250$	scaled by the software		discarded by the software	
	No. of cases	%	No. of cases	%
The operator did not scale the MUF	3	16.7	170	66.9
The operator scaled the MUF	15	83.3	84	33.1
Total	18		254	

Table 1: The performance of the algorithm for rejecting ionograms with insufficient information for different Ct in the oblique ionograms recorded on the Rome-Chania radio link.

	$C_t = 150$	scaled by the software and the operator	
		No. of cases	%
(a)	Accurate	30	37.04
	Acceptable	79	97.53
	Total	81	

	$C_t = 175$	scaled by the software and the operator	
		No. of cases	%
(b)	Accurate	25	37.31
	Acceptable	67	100.0
	Total	67	

	$C_t = 200$	scaled by the software and the operator	
		No. of cases	%
(c)	Accurate	21	38.18
	Acceptable	55	100.0
	Total	55	

	$C_t = 225$	scaled by the software and the operator	
		No. of cases	%
(d)	Accurate	12	34.29
	Acceptable	35	100.0
	Total	35	

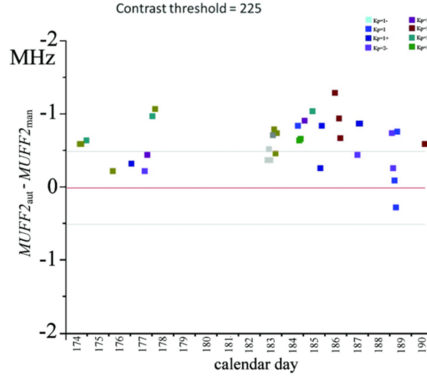|	$C_t = 250$	scaled by the software and the operator	
		No. of cases	%
(e)	Accurate	4	26.67
	Acceptable	15	100.0
	Total	15	

Table 2: Accurate and acceptable values from the test carried out with different C_t in oblique ionograms recorded on the Rome-Chania radio link.
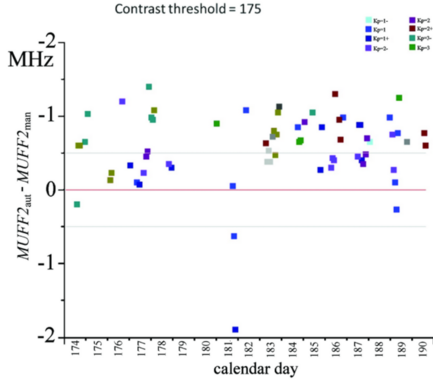
(a) Ct=175
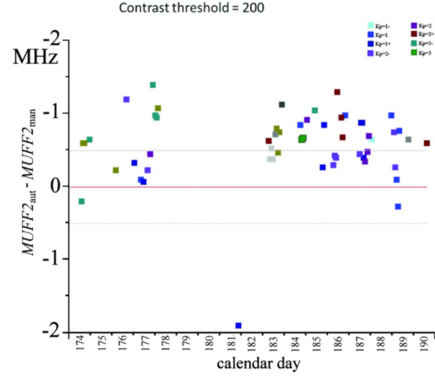
(b) Ct=200

(c) Ct=225

Figure 11: Time scale plot of the difference between autoscaled MUFs and manually scaled MUFs for three different C_t . The colors represent the different values of K_p index associated to each autoscaled ionogram. The number of autoscaled ionograms depends only on C_t and not on K_p.

To study the behavior of the program under different geomagnetic conditions, the algorithm was tested on the same ionogram data set considering different geomagnetic K_p indexes associated to each analyzed oblique ionogram. Using three different contrast threshold values and different geomagnetic K_p indexes, it can be seen that for higher contrast threshold values the number of false positive events decreases, but program performance is not influenced by changing K_p values: as seen in the time series plots on Figure 11, in which the colors represent the different values of the K_p index associated to each ionogram, the number of autoscaled ionograms only depends on the contrast threshold value. This demonstrates good performance of the autoscaling algorithm under different geomagnetic conditions.

These first important results demonstrate how this algorithm for automatic scaling of oblique ionograms can be very useful for analyzing very large data sets of ionograms. This also suggests that it could be applied to any ionospheric oblique soundings irrespective of geomagnetic conditions, ionosonde type, or radio link.

References

[1] Ding, Z., Ning, B., Wan, W., *REAL-TIME AUTOMATIC SCALING AND ANALYSIS OF IONOSPHERIC IONOGRAM PARAMETERS*, CHINESE JOURNAL OF GEOPHYSICS, Vol.50, No. 4, pp. 837-847, 2007.

[2] Frank-Kamenetsky, A. and Troshichev, O., *A relationship between the auroral absorption and the magnetic activity in the polar cap*, Journal ofAtmospheric and Solar-Terrestrial Physics, 77, 4045, 2012.

[3] Galkin, I. A., Reinisch, B. W., Huang, X. and Bilitza, D., *Assimilation of GIRO data into a real-time IRI*, Radio Science, VOL. 47, RS0L07, doi:10.1029/2011RS004952, 2012.

[4] Galkin, I. A., Khmyrov, G. M., Kozlov, A., Reinisch, B. W., Huang, X. and Kitrosser, D. F., *Ionosonde networking, databasing, and Web serving*, Radio Science, VOL. 41, RS5S33, doi:10.1029/2005RS003384, 2006.

[5] Gilbert, J. D. and Smith, R. W., *A comparison between the automatic ionogram scaling system ARTIST and the standard manual method*, Radio Science, Volume 23, Number 6, Pages 968-974, November-December 1988.

[6] Hargreaves, J. K. and Friedrich, M., *The estimation of D-region electron densities from riometer data*, Annales Geophysicae, 21: 603613, 2003.

[7] Herman, J. R., *Spread F and Ionospheric F-Region Irregularities*, REVIEWS OF GEOPHYSICS, VOL.4 , No. 2, MAY 1966.

[8] King, G. A. M., *Spread-F on ionograms*, Journal of Atmospheric and Terrestrial Physics, Vol. 32, pp. 209-221, 1970.

[9] Lastovicka, J., *A3 IONOSPHERIC ABSORPTION MEASUREMENTS AT 1538 kHz - FIRST RESULTS*, Studia geoph. et geod., 22, 1978.

[10] MacDougall, J. W., Hall, G. E., Hayashi, K., *Fregion gravity waves in the central polar cap*, Journal of Geophysical Research, vol. 102, no. A7, pp14,513-14,530, July 1970.

[11] Pendorf, F., *A spread-F index*, J. Geophys. Res. , 1962.

[12] Scotto, C. and Pezzopane, M., *A Software for Automatic Scaling of foF2 and MUF(3000)F2 from Ionograms*, Proceedings of the XXVII General Assembly of the International Union of Radio Science, 1724, Maastricht, The Netherlands, August 2002.

[13] Scotto, C. and Pezzopane, M., *Automatic scaling of polar ionograms*, Antarctic Science, doi:10.1017/S0954102011000587, 2011.

[14] Stankov, S. M., Jodogne, J., Kutiev, I., Stegen, K. and Warnant, R., *Evaluation of automatic ionogram scaling for use in real-time ionospheric density profile specification: Dourbes DGS-256/ARTIST-4 performance*, ANNALS OF GEOPHYSICS, 55, 2, doi: 10.4401/ag-4976, 2012.

[15] Tsunoda, R. T., *Satellite traces: An ionogram signature for large-scale wave structure and a precursor for equatorial spread F*, GEOPHYSICAL RESEARCH LETTERS, VOL. 35, L20110, doi:10.1029/2008GL035706, 2008.

[16] Uemoto, J., Kubota, M., Maruyama, T. and Ishii, M., *Automatic Scaling of Echo Traces on Ionogram: An Attempt to Separate Propagation Modes*, Journal of the National Institute of Information and Communications Technology, Vol.56, Nos.1-4, 2009.

[17] Wright, J. W. and Conkright, R. O., *RESCUING IONOGRAM FILM ARCHIVES AT WORLD DATA CENTERS FOR THE IRI AND POSTERITY*, INAG Report, 63: 30-35, 2002.

[18] Zuccheretti, E., Tutone, G., Sciacca, U., Bianchi, C. and Baskaradas, J. A., *The new AIS-INGV digital ionosonde*, Annals of Geophysics, vol. 46, N. 4, 2003.

6 An Evaluation of Electron Density Along a Transmitter-Receiver Path

In addition to automatic interpretation of oblique ionograms, the object of this work is to achieve determination of electron density of the ionosphere between a transmitter and receiver using oblique ionospheric soundings, with the future goal of real-time evaluation of the ionospheric electron density profile. The basic idea is to start from automatic interpretation of oblique ionograms, then, using an analytical electron density profile to model the ionospheric layers, to perform a ray tracing procedure to calculate a synthetic ionogram. This procedure will simulate the ray path between the transmitter and receiver for each HF frequency (Reilly, M. H.,1991). Measuring the time delay for each frequency provides a synthetic oblique ionogram for comparison with the measured one. The input values of the ionospheric model are changed in a reiterative process until the simulated ionogram matches the measured one.

The first step involves identifying the traces of the oblique ionogram. This is the same as knowing the time taken by a radio wave to travel through a channel between a transmitter and receiver, at least for certain frequencies. These time delays observed in an oblique ionogram can be used to try and determine the most compatible electron density distribution, using a ray tracing algorithm to reconstruct the ray path for each frequency in the HF range. As explained above, the length variations of the physical parameters of ionospheric plasma are typically much smaller than the wave lengths considered, so a geometrical optical approach is useful to describe the ray propagation. Ray tracing is a method that makes it possible to integrate the appropriate ray equations and calculate the path of an electro-magnetic wave travelling through the different ionospheric layers, simulating any absorption, refractions, or reflections. It is clear that a model of the medium through which the ray is travelling is necessary for a ray tracing algorithm in order to calculate the direction of the radio wave at each stage of integration along the path.

This problem is approached in this work using an adaptive model with free parameters p_i $(i = 1, ..., n)$, capable of describing a wide set of radio propagation conditions in the channel between the transmitting station and receiver of the oblique ionogram in question. The basic idea of the proposed procedure consists in choosing the particular distribution of electron density associated to the simulated ray path that best matches the observed time delays. The parameters p_i of the model are varied into appropriate ranges Dp_i centred in the neighbourhood of certain values p_i [base] referred to as base values. Initially these may be modeled according to the helio-geophysical conditions and the information obtained from the identified trace, assuming that the radio link is established due to reflection from a single layer. A large set of profiles is obtained in this way, and from these a corresponding set of

simulated oblique ionograms. The algorithm selects the ionogram from among those most similar to the recorded one. The initial numerical experiments for the present study were carried out imposing some simplifications regarding both ray-tracing and the adaptive model.

6.1   An Analytical Model of the Ionosphere

Oblique ionospheric radio soundings are performed with the transmitter and receiver located at widely varying distances, typically in the order of a thousand kilometers. For example, the oblique ionograms used here are from the Rome-Chania radio link, a distance of about 1225 Km. It is obvious that an adaptive model capable of describing variations in electron density over distances of this magnitude must also take latitudinal and longitudinal variations in the ionosphere into account. In this preliminary study, however, a model of electron density profile was adopted that ignores these variations. It derives from the profile used in Autoscala (Scotto C., 2009) and it is summarized as follows, with reference to Figure 12. The bottom-
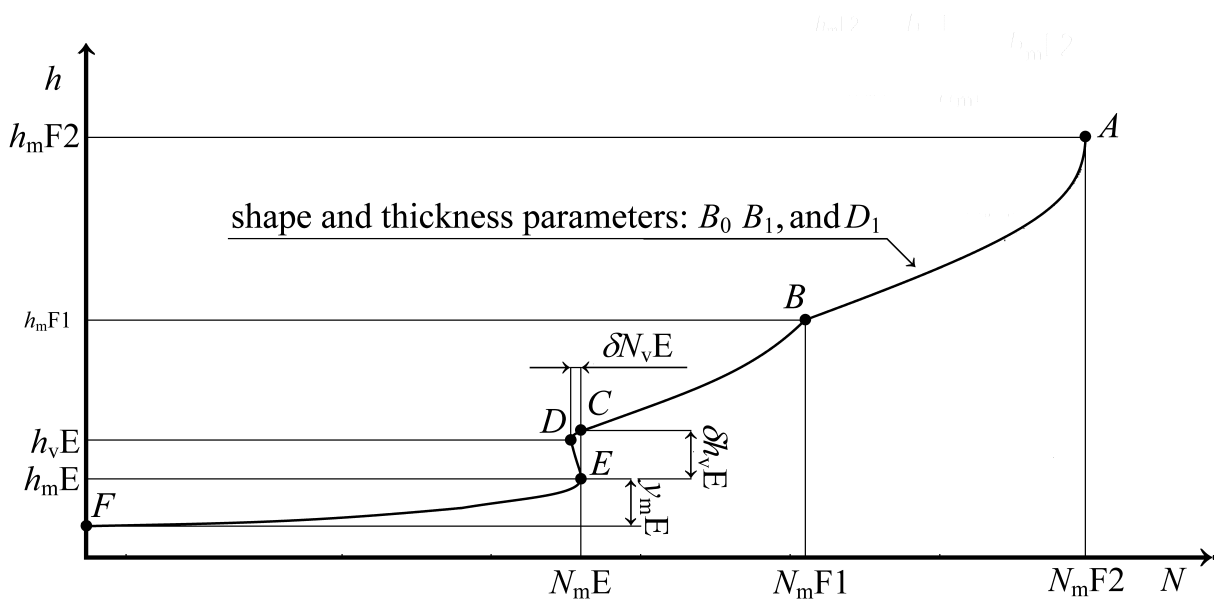
Figure 12: The model electron density profile used in this work. It is based on 12 free parameters and is derived from the one used in the Autoscala software (Scotto, 2009).

side F_2 profile and the F_1 layer are constructed on the basis of the formulation for the representation of the F_1 layer in the International Reference Ionosphere (IRI)

electron density profile of Reinisch and Huang (2000). The E region is modelled by defining the position of four anchor points (see Figure 12). Point C is joined to point D by a parabola. Point D is joined to point E by a cubic curve. The bottom-side of the E region (from point E to point F) is modelled by a parabolic layer (Bilitza, D., 1998). The electron density profile model is constructed from 12 free parameters (6 related to the E region, and 6 to the F_2 F_1 layers):

1) N_mF_2 maximum electron density of F_2 layer;
2) h_mF_2 height of maximum electron density of F_2 layer;
3) N_mF_1 maximum electron density of F_1 layer;
4) B_0 thickness parameter;
5) B_1 shape parameter;
6) D_1 shape parameter;
7) N_mE maximum electron density of the E layer;
8) h_mE height of maximum electron density of E layer;
9) h_vE height of the E valley point;
10) δh_vE E valley width;
11) δN_vE E valley depth;
12) y_mE parabolic E layer semi-thickness.

Although this model is in some respects very simple and ignores the horizontal gradients of the ionosphere, it is suitable for its intended purpose. It is highly adaptive, providing a different $N(h)$ for each combination of the input parameters described above, which can be chosen within very wide intervals, providing an adequate representation of any reasonable ionosphere.

6.2   Eikonal Based Ray Tracing Procedure

As already mentioned, oblique ionograms are useful for studying free electron distribution along a ray path. To achieve this, an eikonal based ray-tracing was performed (Borovskikh, A. V., 2010), considering the ionosphere as characterized by a slowly varying refractive index that gradually changes only in its vertical component. This means considering a medium in which the absolute dielectric constant ϵ, magnetic permeability, μ and conductivity σ slowly vary in space. Since the variations in the medium have a much smaller scale length than the wavelengths in question, the ionosphere is approximated to a homogeneous isotropic medium (Bianchi, C. and Bianchi, S., 2009). Under these assumptions, the eikonal equation is:

$$|\nabla S| = n \tag{23}$$

which describes phase spatial variations in relation to the refraction index. The solution of this equation gives the eikonal function $S(r)$. The idea is to determine the ray equation in relation to the refractive index distribution $n(\vec{r})$. Initially $\hat{s}(\vec{r})$ is considered as the versor, identifying the local propagation direction of the ray

$$\hat{s}(\vec{r}) = \frac{\nabla S(\vec{r})}{|\nabla S(\vec{r})|} = \frac{\nabla S(\vec{r})}{n(\vec{r})} \tag{24}$$

introducing the curvilinear coordinate of the ray

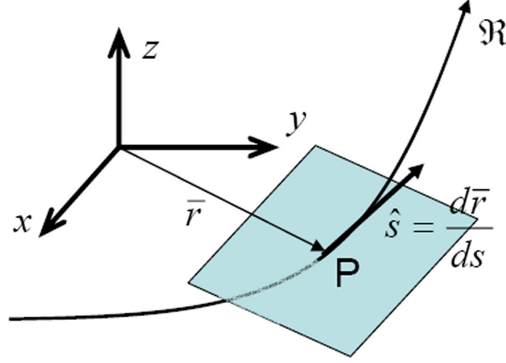$$s(P) = \int_{P_o}^{P} \sqrt{dx^2 + dy^2 + dz^2} \tag{25}$$
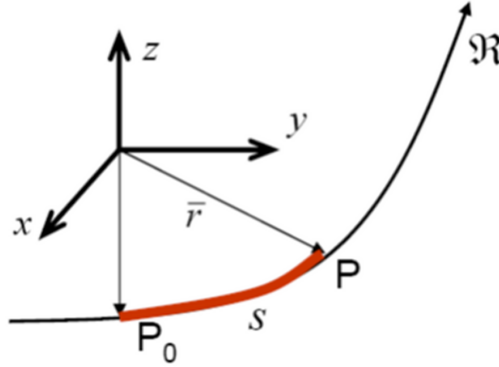
and considering the tangent versor of the ray in a generic point, gives:

$$\hat{s}(s) = \frac{dx\hat{x} + dy\hat{y} + dz\hat{z}}{\sqrt{dx^2 + dy^2 + dz^2}} = \frac{d\vec{r}(s)}{ds} \tag{26}$$

where $\vec{r}(s)$ is the parametric equation of the trajectory, then:

$$n(s)\frac{d\vec{r}(s)}{ds} = \nabla S(s) \tag{27}$$

which represents the ray equation. Deriving the ray equation relative to s produces the differential ray equation:

$$\frac{d}{ds}(n\frac{d\vec{r}}{ds}) = \nabla n \tag{28}$$

In this case the Earth's magnetic field is ignored and only the ordinary trace of the oblique ionogram is considered. The ray tracing program evaluates the time delay of a number of frequencies in the HF range, integrating the equation (28) and obtaining a ray path for each frequency of the electromagnetic HF waves, in relation to the refractive index variations $n(\vec{r})$.

For each step of integration, the ray path of the relative HF radio wave is calculated through the ionosphere. The refraction index is calculated with the Appleton-Hartree formula, ignoring the Earth's magnetic field and collisions

$$n = \sqrt{1 - \frac{\omega_p^2}{\omega^2}} \tag{29}$$

where ω_p is the plasma frequency ($\omega_p^2 = \frac{Ne^2}{m_e\epsilon_0}$). In the Earth's ionosphere, the free electron density varies between 10^4 and 10^6 $electrons/cm^3$, corresponding to a plasma frequency on the order of $w_p \sim 6\mathrm{x}10^6 \div 6\mathrm{x}10^7\ sec^-1$. One of the most difficult and important parts of any ray-tracing algorithm is what is called the homing-in procedure. This procedure makes it possible to establish the path from the transmitter to the receiver, for each HF radio wave considered. Since eikonal based

ray-tracing is used to calculate the ray path for a radio link of 1225 Km, any ray path that does not connect the transmitter to the receiver must not be taken into account and discarded. The adopted homing-in method was also appropriate for use in the presence of ionospheric gradients or ripples, similar to the one proposed by Strangeways (2000). In this method both initial elevation and azimuth are automatically adjusted to find the path that arrives exactly at the receiver, as shown in Figure 13. The procedure begins by launching a simulated ray with an inclination close to 90° to the ground ,after being refracted as it passes through the ionospheric layers, it might or might not be reflected.

If the radio frequency is smaller than the plasma frequency of the ionospheric layer, the electromagnetic wave is not reflected: the radio wave is then automatically re-transmitted by the program at a different elevation angle, smaller than the previous one. In case of a phase refractive index $\mu_f = \frac{c}{v_f} = c\frac{k}{\omega} = 0$ the radio wave is reflected by the ionosphere and returns to the ground. The high frequencies proximal to the MUF have two different propagation channels, one reflected at a higher virtual high than the other. This is the peculiarity that gives an oblique ionogram its typical "nose" shape. If the highest ray-path of the HF signal is simulated and it is reflected to the ground at a distance greater than the distance between transmitter Tx and receiver Rx, the radio wave is automatically re-launched at a smaller angle. If the distance reached by the highest ray is less than that between Tx and Rx, the radio wave is automatically re-launched at an angle greater than the previous one, but smaller than the angle for which the distance on the ground is greater than the distance between transmitter and receiver. The same kind of procedure is applied for the lower ray path of the HF signal in question.

The homing method described can also be used in the presence of ionospheric gradients or ripples and for any 3D ionospheric model to find precise ray paths and group delays. Time delays were calculated by integrating

$$t = \frac{1}{c} \int_0^{h_r} \frac{dh}{n} \tag{30}$$

on the selected ray path. In this way, $h' = c * t$ is obtained for each HF frequency in question, achieving a simulated oblique ionogram.

The ray tracing software reads the analytical electron density profile, which provides the input values for the program, and then starts simulating the ray paths that join the virtual transmitter and virtual receiver for frequencies from 2 to 30 MHz. Once the relative time delay has been calculated for each path, an oblique synthetic ionogram is provided as output.
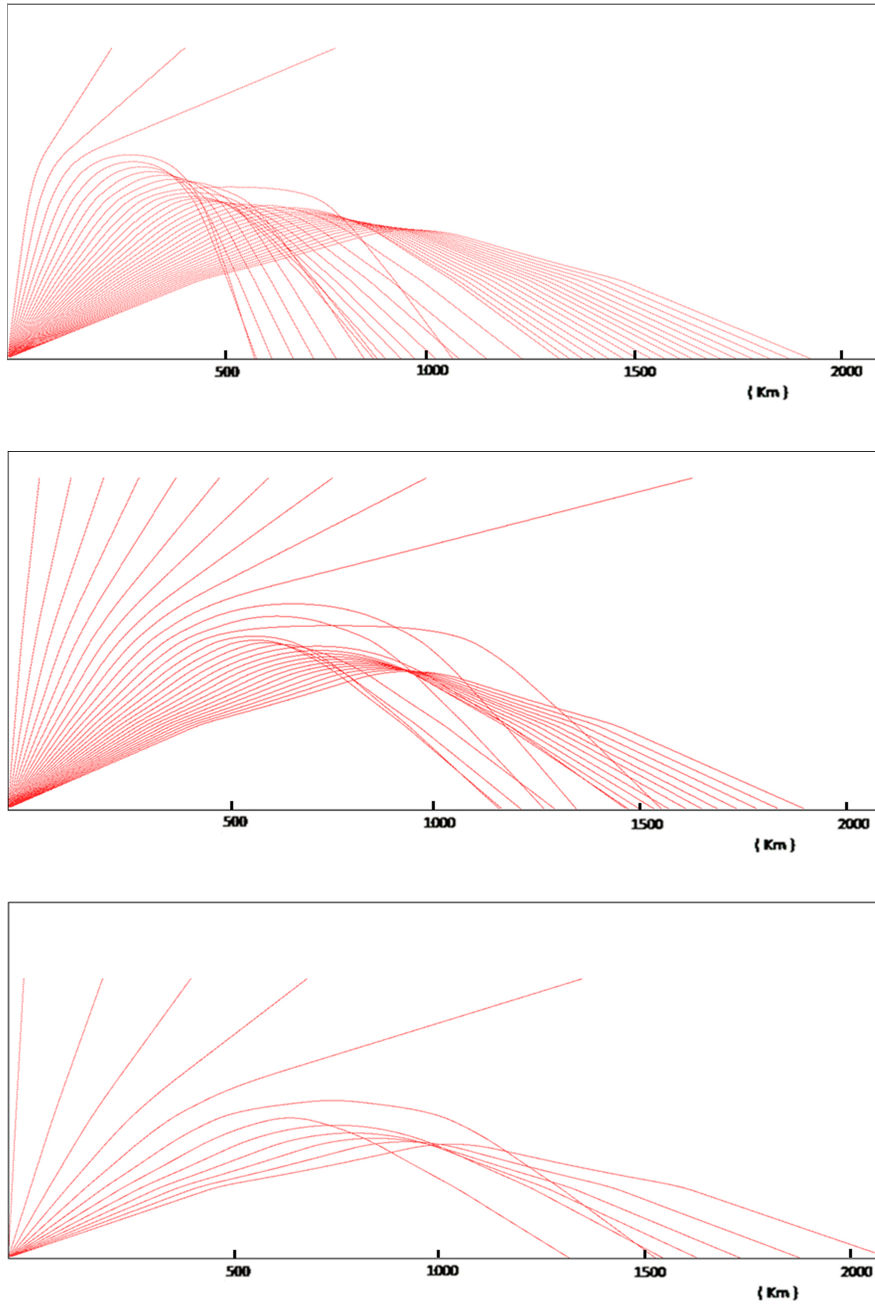
Figure 13: The upper panel shows a ray tracing for a HF radio wave at the frequency of 10 MHz. The middle panel shows a ray tracing for a HF radio wave at the frequency of 14 MHz. The lower panel shows a ray tracing for a HF radio wave at the frequency of 24 MHz.

## 6.3 Adaptation Techniques for Ionospheric Model Parameters

The synthetic ionogram produced by the ray tracing algorithm, is then compared to the measured one, matching the time delays for each frequency. As shown in Figure 14, if the difference between the time delay values of the two oblique soundings is less than a threshold Δt fixed at $0.05ms$, the electron density profile used in the ray tracing program is considered as a realistic model of the electron distribution along the ray path and its physical parameters are taken as representative of the ionospheric region between the transmitter and the receiver. Otherwise the simu-
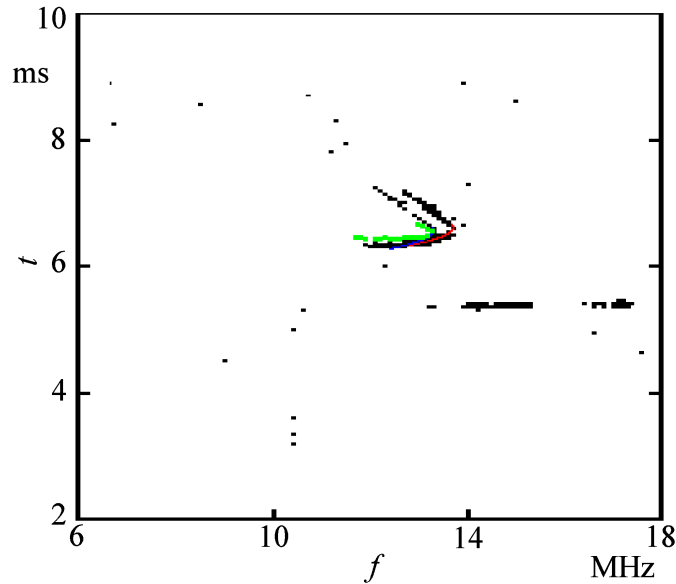
Figure 14: An oblique ionogram recorded on the Rome-Chania radio link on June 25, 2011, at 10:00. The trace was restored applying a ray-tracing procedure based on the integration of the eikonal equation. The electron density profile, which is considered the same throughout the channel between transmitter and receiver, is based on the model shown in Figure 8.

lated oblique ionogram is discarded and the electron density profile is not considered as representative of the ionospheric conditions in the region traversed by the radio wave. In this case the profile parameters are automatically changed and a new ray tracing procedure begins with the new electron density profile. The entire procedure is repeated until the synthetic oblique ionogram matches the measured one, as explained above and shown in the flowchart of Figure15.

In the example of Figure 14, of an oblique ionogram recorded on the Rome-Chania

44
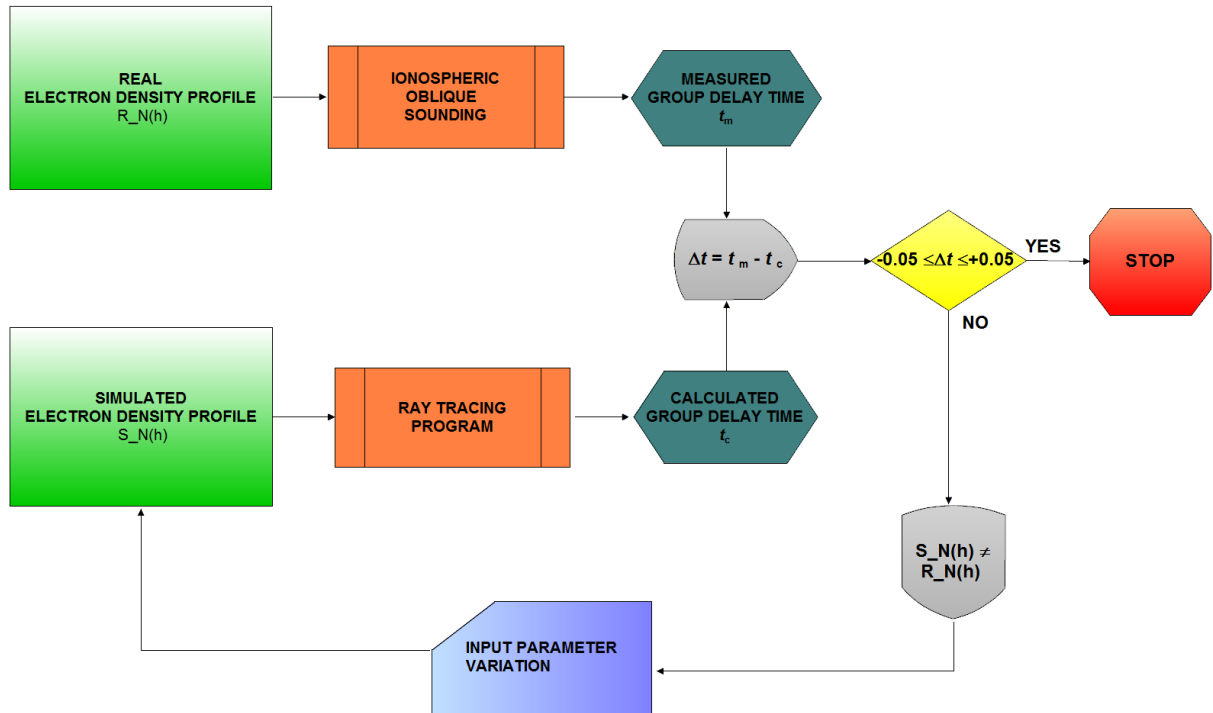
Figure 15: A flow chart for the process of reconstruction of the electron density profile between a transmitter and receiver using the eikonal based ray tracing program.

radio link on June 25, 2011, at 10:00, It can be seen that the program in this case correctly identified the trace of the ionogram. On the basis of three points from the identified trace, the electron density profile was adapted so that the trace of the observed ionogram was restored by ray-tracing. This profile, according to the characteristics of the ionospheric model applied, was assumed to be the same all along the path between the transmitter and receiver.

References

[1] Bianchi, C. and Bianchi, S., *PROBLEMA GENERALE DEL RAY-TRACING NELLA PROPAGAZIONE IONOSFERICA - FORMULAZIONE DELLA RAY THEORY E METODO DEL RAY TRACING*, Rapporti Tecnici INGV, No. 104, 2009.

[2] Bilitza, D., *Improving the standard IRI B0 model*, Proceedings of the IRI Task Force Activity 1997, Report IC/IR/98/9, 614, International Center for Theoretical Physics, Trieste, Italy, 1998.

[3] Borovskikh, A. V., *EIKONAL EQUATIONS FOR AN INHOMOGENEOUS ANISOTROPIC MEDIUM*, Journal of Mathematical Sciences, Vol. 164, No. 6, 2010.

[4] Reilly, M. H., *Upgrades for efficient three-dimensional ionospheric ray tracing: Investigation of HF near vertical incidence sky wave effects*, Radio Science, Vol. 26, N. 4, pp. 971-980, July-August 1991.

[5] Reinisch, B. W. and Huang, X. *Redefining the IRI F1 layer profile*, Advances in Space Research, vol. 25, Issue 1, pp. 8188, 2000.

[6] Scotto, C., *Electron density profile calculation technique for Autoscala ionogram analysis*, Advances in Space Research, 44, pp. 756766, 2009.

7 Automatic Scaling of IPS Oblique Ionograms

The Ionospheric Prediction Service (IPS) of the Australian Bureau of Meteorology is a high profile research institute in ionospheric studies. The main aim of the institute is space weather monitoring and forecasting, which includes studying solar activity, and geophysical and ionospheric conditions. It also provides support for a wide range of systems and technologies affected by space weather, such as HF radio systems, communications, and surveillance systems. The Australian research institute for ionospheric studies manages an extensive network of observatories with magnetometers, ionosondes, and other sensors within the Australia-New Zealand region and Antarctica. The IPS provides information about space weather in daily, weekly, or monthly reports with alerts and warnings when required by the space weather conditions. The space weather and ionospheric forecasts are based on the study of an enormous quantity of data obtained from ionosondes in the Australian and New Zealand network (Terkildsen and Neudegg, 2014).

The autoscaling algorithm described above was applied to the ionograms produced by the Australian ionosonde network, since the IPS ionospheric databases contain a huge number of oblique ionograms taken along numerous different ray paths. Over 4000 oblique ionograms produced by many different ionosondes in the Australian territory were analyzed.

7.1 Setting the Automatic Scaling Software

As already explained, the algorithm for the automatic interpretation of oblique ionograms needs to be set for each particular radio link. Every individual ray path is characterized by different physical ionospheric parameters, so oblique ionograms from a particular radio link carry all the information about the ionospheric portion between the transmitter and receiver in question. Furthermore, the type of ionosonde used for the oblique soundings has to be taken into account, since the autoscaling program is based on a image recognition process and each ionosonde gives a different image for the oblique ionogram. Image characteristics like ionogram brightness, thickness of trace, and ionogram background noise (Neudegg, D., 2001) are important parameters that the autoscaling algorithm needs to be set for. This is critical and not as simple as it might seem: the local correlation between the branches of analytical parabolas and the ionogram trace pixels, which is the main focus for the contrast method used in automatic scaling, is strongly influenced by the properties of the image representing the ionogram. Based on the Visual Basic program for the INGV oblique ionogram automatic scaling system, an IDL code, of more than 800 program lines, was implemented in order to adapt the autoscaling algorithm to the IPS oblique soundings. The autoscaling program was trained us-

Figure 16: The three radio links studied in Australian territory. The red line represents the Kalkarindji - Culgoora radio link (2380 Km); the blue line represents the Lynd River - Culgoora radio link (1450 Km); the yellow line represents the Curtin - Culgoora radio link (2960 Km).

ing three different radio links, setting the algorithm for a wide range of ionospheric conditions:

1)Kalkarindji, Australia $(17.43S, 130.81E)$ - Culgoora, Australia $(30.30S, 149.55E)$;
2)Lynd River, Australia $(18.25S, 144.87E)$ - Culgoora, Australia $(30.30S, 149.55E)$;
3)Curtin, Australia $(17.60S, 123.82E)$ - Culgoora, Australia $(30.30S, 149.55E)$.

The first from Kalkarindji to Culgoora is indicated with a red line in Figure 16, and is a radio link of 2380 Km. The second from Lynd River to Culgoora is indicated with a blue line, and is 1450 Km. The third from Curtin to Culgoora is indicated with a yellow line and is 2960 Km.

The IPS oblique ionograms were recorded using a Digital Oblique Receiving System (DORS) on loan from the Australian Defence Science and Technology Organisation (DSTO). The ionograms produced by the IPS ionosondes were PNG images, as shown in the left panel of Figure 17. Following the same procedure as for the INGV oblique soundings, the Australian oblique ionograms were first recorded in a matrix form, with m rows $m = int[(t_1 - t_0)/\Delta t)] + 1$ and n columns $n = int[(f_1 - f_o)/\Delta f)] + 1$,
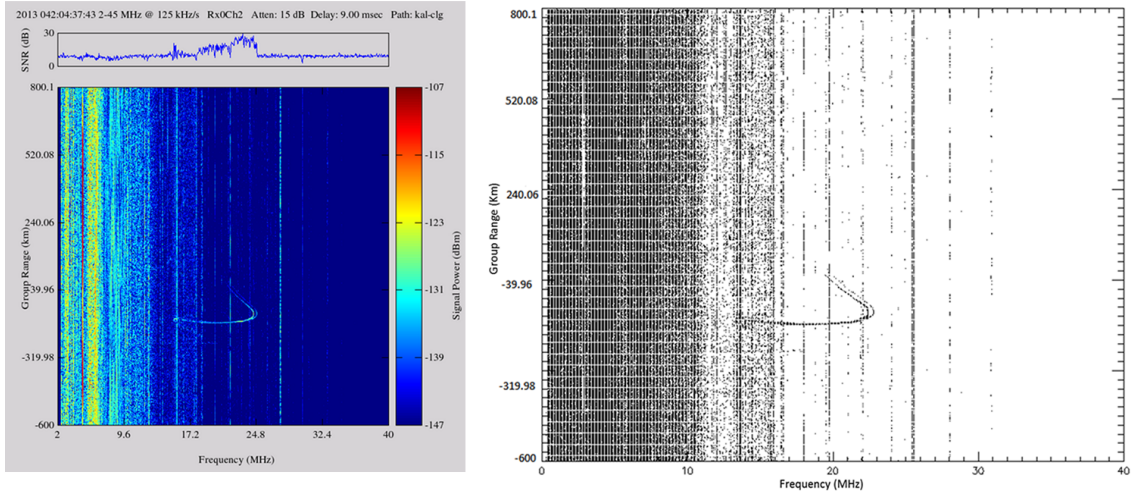
Figure 17: The left panel shows a PNG ionogram image recorded by the IPS ionosondes on February 11, 2013 from the Kalkarindji - Culgoora radio link. The right panel shows the same ionogram converted into matrix form and plotted.

and then plotted as seen in the right panel of Figure 17. Also in this case, the element a_{ij} (with $i = 1, ..., m$ and $j = 1, ..., n$) of the matrix A, which is an integer ranging from 0 to 255, is proportional to the amplitude of the received echo.

One of the most problematic issues in automatic interpretation of oblique ionograms is distinguishing the characteristic traces of the oblique soundings from the background noise pixels that often affect the images. In the example of Figure 17 the presence of dense noise represents a significant problem to be solved in order to permit automatic scaling of the ionogram. Since this autoscaling method is based on the correlation between the two analytic branches of parabola and the ionogram trace pixels, the RF noise disturbing the ionogram can affect the validity of automatic scaling. Every pixel that is not part of the information on the the ionospheric parameters contained in the ionogram, could generate incorrect output data.

To reduce the RF noise without eliminating relevant ionogram features, an additional algorithm was developed to filter most of the background noise from the image without affecting the significant information of the oblique ionogram. This filter algorithm analyses a certain number of pixels adjacent to each pixel in turn. Image background noise is often present as a dense set of pixels, and so when the number of pixels in the neighborhood of the pixel being analyzed is greater than a set threshold, the pixel in question is assumed to be part of the noise and then deleted. Once implemented in the automatic scaling program, the result of the filter algorithm can be seen in Figure 18, showing the same ionogram as Figure 17 after filtering for background noise and automatic scaling.

49

The IDL code was set using a group of 40 ionograms from the above three differ-
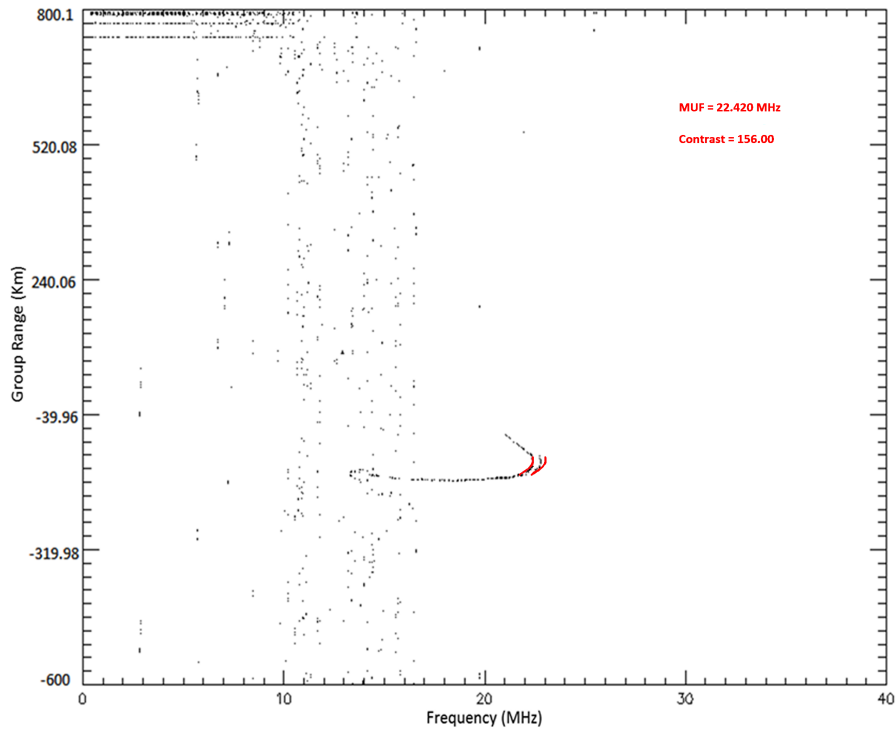
Figure 18: An oblique ionogram recorded on February 11, 2013 on the ray path between Kalkarindji and Culgoora, filtered for background noise and autoscaled by the software. As can be seen the analytic curves, here in red, closely fit the typical shape of the ordinary and extraordinary trace.

ent radio links. After establishing what appeared to be a good parameter for the application of the contrast method for effective interpretation of the IPS oblique ionograms, the algorithm was tested on a larger set of ionograms. 606 oblique iono- grams were analyzed by the software, 202 for each of the three radio links. Before running the autoscaling program, all the 606 ionograms were scaled by an expert operator, who discarded the ionograms that could not be interpreted due to lack of data or excessive background noise, and assigned MUF values for the remainder. Besides interpreting ionograms to generate an output MUF value for each one, the other main and probably most important issue of an autoscaling algorithm is being able to discard ionograms that even an expert operator could not interpret. This is critical for automatic interpretation of oblique ionograms, in order to avoid incorrect output data. This is why the oblique sounding data set chosen for the test includes low quality ionograms so as to train the program to distinguish ionograms to be

50

discarded from those with sufficient information for scaling. As already explained, the contrast method used to recognize the ordinary and extraordinary traces of ionospheric soundings is also a useful method for discarding ionograms lacking data or excessively noisy. As in the interpretation of the INGV data, once a threshold value was set for contrast C_t, only when C_{max} is above than this value, the resulting analytic curves are considered representative of the traces due to reflection from the F2 region, as can be seen in the example in Figure 18. Otherwise, no MUF value is provided as output and the ionogram is deemed to lack sufficient information and discarded. Testing established that using a contrast threshold of 50, the program performs well, identifying real traces and discarding ionograms that lack data. For all the three radio links considered, an agreement of more then 80% was observed between manual scaling of an expert operator and automatic scaling by the software.

7.2   Performance of the Autoscaling Software

During this stage, a larger set of data from an oblique sounding campaign between the Kalkarindji and Culgoora ionosondes was considered. In order to rigorously test of the algorithm, 2880 oblique ionograms were analyzed, including ionograms outside the restricted database used to set C_t. Once again an expert operator interpreted the data first, establishing that the quality of the ionograms was relatively low, and in only 1007 out of 2880 was he was able to establish the MUF with an accuracy of 0.5 MHz, while in 1873 out of 2880 ionograms it was not possible to establish the MUF. Using a C_t value of 60, the results obtained from the autoscaling software were compared to manual scaling and are reported in Table 3. Once again a distinction was made between the autoscaled ionograms, defining as "accurate" those for which the MUF value was autoscaled with an accuracy of 0.5 MHz, and "acceptable" when the accuracy was within 1.5 MHz. Even though more than 50% of the ionograms could not be manually scaled because of RF noise or lack of data, the results, as can be seen in Table 3, demonstrate the good performance of the autoscaling program, which agrees in more than 80% of cases with the interpretation provided by the operator. It is also worth noting that the analysis of the ionogram and autoscaling operations take less then two minutes for each oblique sounding, which is a very reasonable computation time for this kind of procedure.
Table 3(a) shows that, as in the manual scaling, a high percentage of ionograms lacked recognizable traces were discarded, while the ionograms with well defined traces were all correctly autoscaled, in spite of the low quality of the data set used. However, the presence in the database of a large number of low quality ionograms, makes it possible to efficiently assess the rejection capabilities of the program. This is why a number of false positive events, like the example shown in Figure 19, were
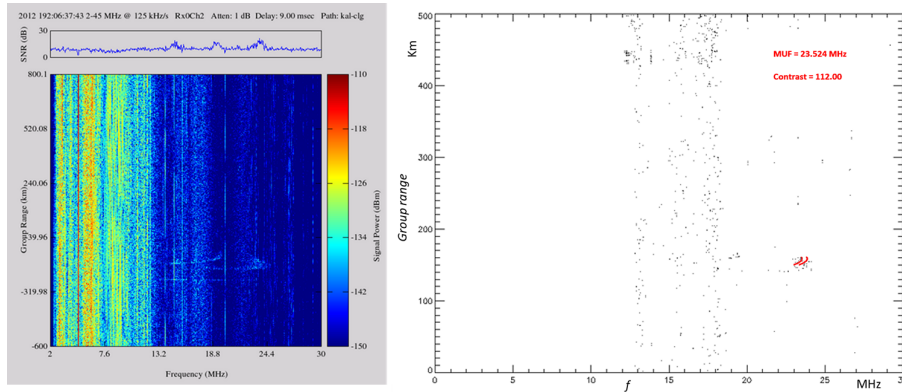
$C_t = 50$	scaled by the software		discarded by the software	
	No. of cases	%	No. of cases	%
The operator did not scale the MUF	194	18.8	1679	90.1
The operator scaled the MUF	840	81.2	167	9.0
Total	1034		1846	

(a)

$C_t = 50$	scaled by the software and the operator	
	No. of cases	%
Accurate	760	90.5
Acceptable	840	100.0
Total	840	

(b)

Table 3: Table 3(a) reports the performance of the algorithm for rejecting ionograms with insufficient information using $C_t = 50$ on the oblique ionograms recorded on the Kalkarindji-Culgoora radio link. Table 3(b) reports accurate and acceptable values for the tests carried out with $C_t = 50$ on the oblique ionograms recorded on the Kalkarindji-Culgoora radio link.

generated by the software. This constitutes the most critical issue for the autoscaling procedure and is a major problem in space weather applications. It is considered preferable to discard questionable data rather than generate incorrect output. The contrast threshold is the key parameter for rejecting ionograms in which it is not possible to detect a MUF value, and so a second cycle of autoscaling was performed on the same data set of 2880 oblique soundings, using this time a higher contrast threshold: $C_t = 60$. Table 4 reports the results of the second autoscaling cycle. In this case, the number of ionograms wrongly scaled by the software, in which an operator would not be able to recognize a MUF value, decreases markedly. The percentage agreement between the autoscaling program and manual scaling increases to 84.8%, which represents a very good result considering the low quality of analyzed data. In the results presented in Tables 3-4, it is remarkable that the software provides acceptable values for 100% of the ionograms with well defined traces, representing almost all the ionograms manually scaled by the operator.

A comparison between the MUF values provided by the autoscaling program and those obtained by manual scaling from the same ionogram data set, demonstrates the efficiency of the procedure developed for detecting the typical shape of an oblique ionogram. This offers a very interesting prospect: a computer program that gives real-time evaluation of the MUF for a particular radio link using oblique radio soundings.

Figure 19: An example of a false positive event generated by the autoscaling algorithm. The oblique ionogram recorded on July 10, 2012 was discarded by the operator but not by the software, which generated an incorrect MUF value as output.

In the second autoscaling cycle of the 2880 IPS oblique ionograms, as the contrast threshold increases a greater number of ionograms scaled by the operator were rejected by the software, but conversely the percentage of false positive events decreased considerably. When large quantities of data are analyzed automatically, is preferable to sacrifice a few correct items rather than use potentially incorrect data, which could compromise the modeling. This also is why it is preferable to use a low quality data set for testing any algorithm intended for automatic processing.

After setting the autoscaling program for IPS oblique sounding and training it using a large set of low quality ionograms in order to verify the rejection capabilities of the algorithm, a new database of 384 oblique ionograms were analyzed. The ionograms represent two days of records, the 15 and 16 of April 2013, on a radio link of 1218 Km, from the CUR ($17.60S$;$123.82E$) ionospheric station in Western Australia, to the MTE ($23.48S$;$133.81E$) ionosonde in the Northern Territory of Australia, as shown in Figure 20. The quality of the oblique soundings was very high (Gardiner-Garden et al., 2008) and an expert operator was able to manually scale a MUF value for every ionogram in the data set. The two previous cycles of the program on the 2880 ionogram data set demonstrated that a contrast threshold $C_t = 60$ gives best results in terms of well-autoscaled ionograms versus false positive events. The same C_t value was used for the new data set of high quality oblique soundings. Again the inonograms arrived as PNG images, as shown in the left panel of Figure 21, and were then converted into a matrix form for analysis by the autoscaling software, as shown in the right panel of Figure 21. It can be seen in Figure 21 that even when the quality of the ionogram is high and the two typical traces can be easily recognized in the image, the program's filter algorithm works effectively, giving an

$C_t = 60$	scaled by the software		discarded by the software	
	No. of cases	%	No. of cases	%
The operator did not scale the MUF	109	15.2	1764	81.6
The operator scaled the MUF	610	84.8	397	18.4
Total	719		2161	

	$C_t = 60$	scaled by the software and the operator	
		No. of cases	%
(b)	Accurate	565	92.7
	Acceptable	610	100.0
	Total	610	

Table 4: Table 4(a) reports the performance of the algorithm for rejecting ionograms with insufficient information using $C_t = 60$ on oblique ionograms recorded on the Kalkarindji-Culgoora radio link. Table 4(b) shows accurate and acceptable values for the tests carried out with $C_t = 60$ on the oblique ionograms recorded on the Kalkarindji-Culgoora radio link.

(a)

$C_t = 60$	scaled by the software		discarded by the software	
	No. of cases	%	No. of cases	%
The operator did not scale the MUF	0	0	0	0
The operator scaled the MUF	384	100.0	0	0
Total	384		0	

|	$C_t = 60$	scaled by the software and the operator	
		No. of cases	%
(b)	Accurate	345	89.9
	Acceptable	369	96.1
	Total	384	

Table 5: Table 5(a) reports the performance of the algorithm in rejecting ionograms with insufficient information using $C_t = 60$ on the data set of 384 high quality oblique ionograms recorded on the Australian CUR-MTE radio link. Table 5(b) shows accurate and acceptable values for the tests carried out with $C_t = 60$ on the data set of 384 high quality oblique ionograms recorded on the Australian CUR-MTE radio link.

Figure 20: The red line in the figure shows the radio link between the CUR (17.60S ; 123.82E) and MTE (23.48S ; 133.81E) ionosondes.

even more clearly defined image for calculating the local correlation between the analytical curves and image pixels.

The results of the autoscaling of this high quality oblique sounding data set, demonstrate very close agreement between manual and automatic scaling, as reported in Table 5. None of the 384 ionograms were rejected by the software, in total agreement with manual scaling, as can be seen in the examples of Figure 22. In more than 89% of cases the MUF values provided by the program were within a range of ±0.5 MHz from the values provided by an expert operator, and for more than 96% of the ionograms the MUF values provided by the operator and the software differ by at most ±1.5 MHz, limits compliant with the URSI standard (Piggott and Rawer, 1972). This demonstrates that the number of false positive events drastically decreases as the quality of the analyzed data increases: the percentage of false positive events in this case was 3.9%. This demonstrates that in addition to good performance of the autoscaling algorithm, it is increasingly efficient in discarding oblique ionograms that lack sufficient information as the quality of the data improves. In Figure 23 the MUF values provided by an operator are plotted against the vertex coordinates of the two branches of parabola used as correlation functions in the autoscaling algorithm. The red triangle in the figure is the x coordinate of the vertex of the parabola which reconstructs the ordinary trace of the oblique ionogram and represents the
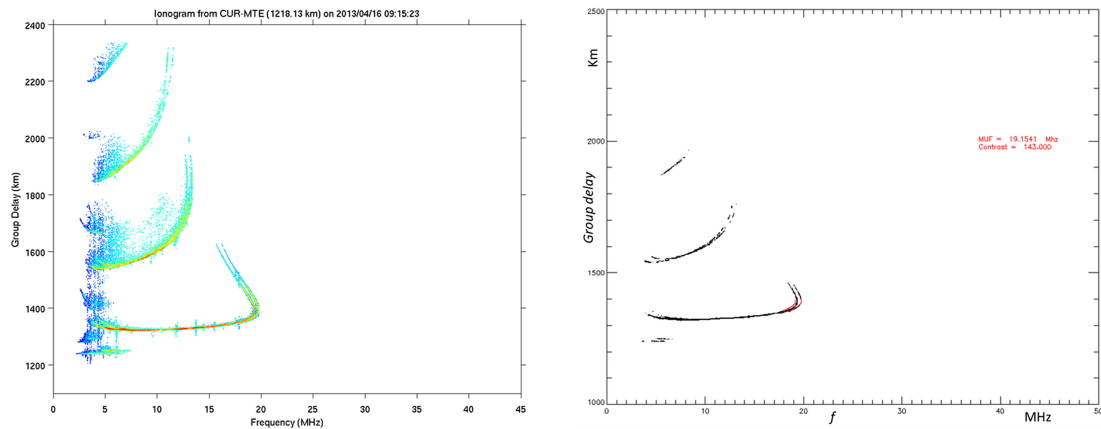
Figure 21: In the left panel it can be seen the ionogram related to the CUR - MTE radio link, taken on 16th April 2013 at $09:15$. The right panel shows the same ionogram after the autoscaling procedure

MUF value provided by the program. A close agreement is clearly seen between manual and automatic scaling.

On the strength of the good results of automatic scaling of oblique ionograms, the program was used by IPS researchers to validate their tool for forecasting MUF values. A month of ionogram data for December 2012 was analyzed by the autoscaling software. The MUF values detected by the program were then compared with the values provided by the IPS MUF prediction tool. The results of this preliminary test were remarkably good and other tests are planned in the future to improve the IPS MUF forecasting tool.
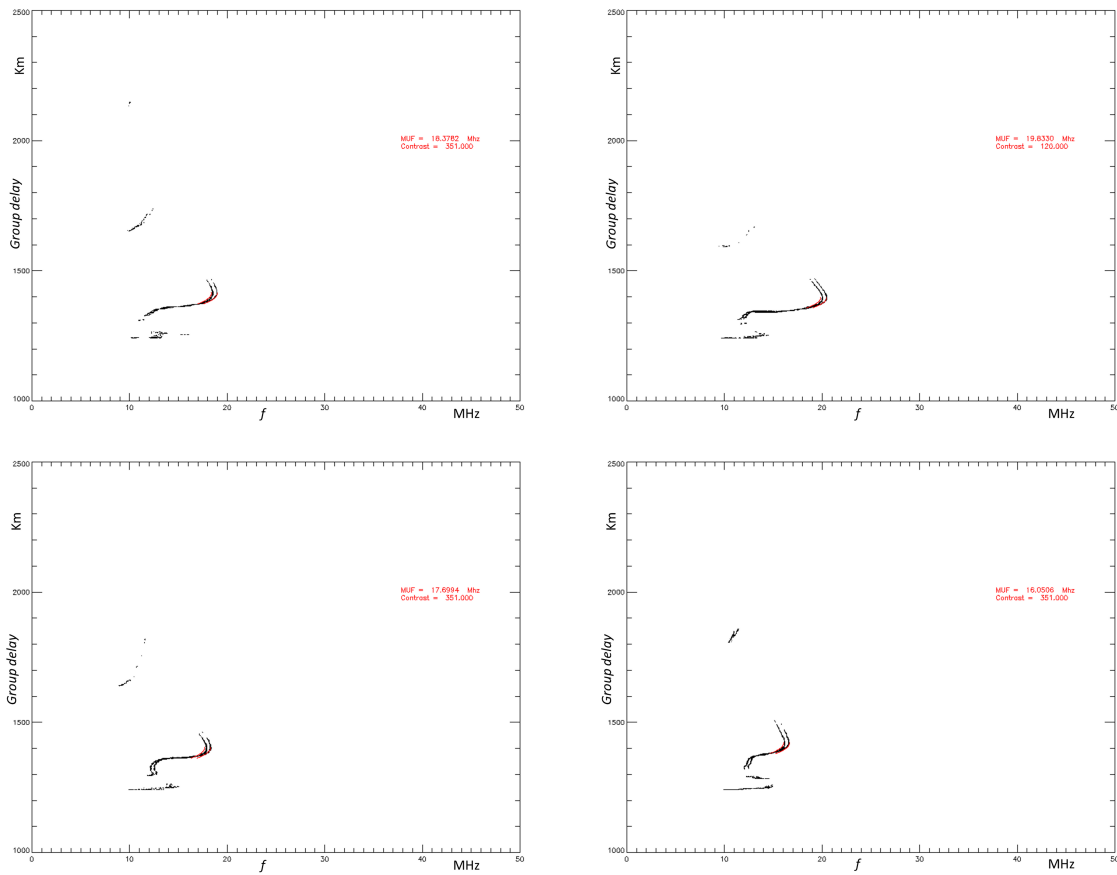
Figure 22: Examples of autoscaled ionograms from the CUR - MTE campaign. For more then the 96% of the analysed ionograms of this campaign both the operator and the software were able to provide the MUF value with an accuracy of ± 1.5 MHz.
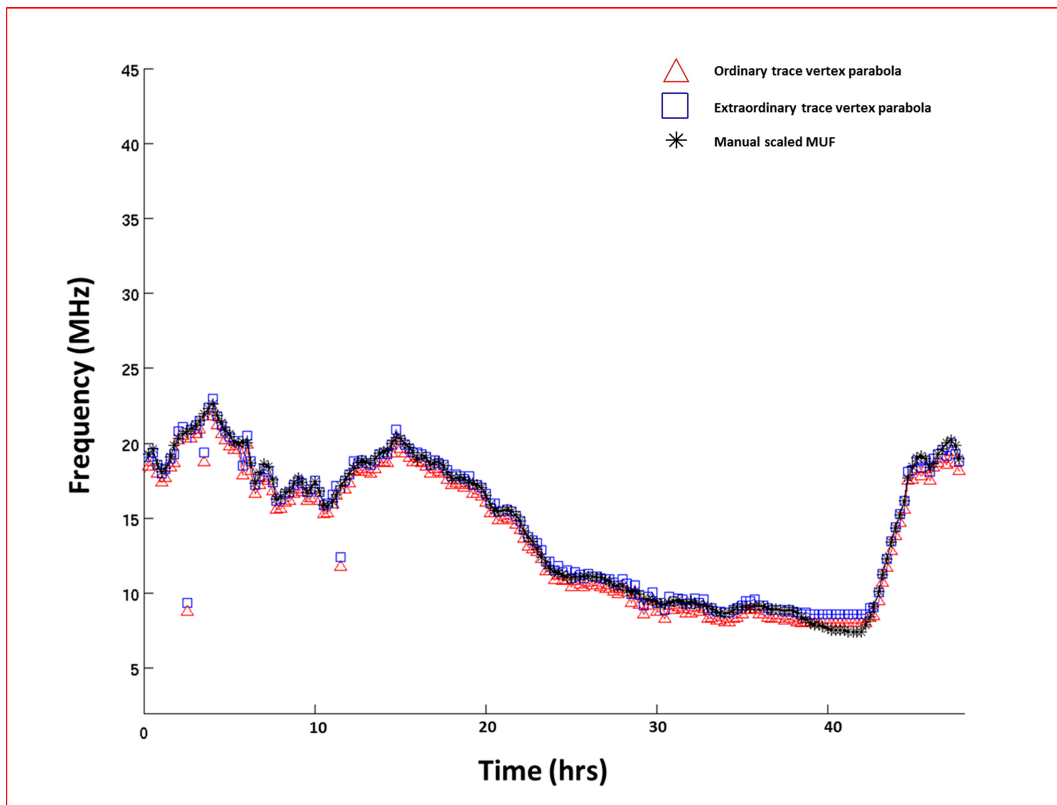
Figure 23: The values of the MUF provided by the operator plotted versus the vertex coordinates of the two analytic curves. The red triangle is the X coordinate of the vertex of the parabola which reconstructs the ordinary trace of the oblique ionogram and represents the MUF value provided by the program.

References

[1] Gardiner-Garden, R., Ayliffe, J., Durbridge, L., Frazer, G., Heitmann, A., Praschifka, J., ... and Turley, M., *A new high-fidelity oblique HF receiving system*, In Proc. IES2008 12th International Ionospheric Effects Symposium, pp482-491, 2008.

[2] Neudegg, D., *Statistical addition method for external noise sources affecting HF-MF-LF systems*, Radio Science, vol. 36, Issue 6, pp. 16591667, 2001.

[3] Piggott, W. R., Rawer, K., *U. R. S. I. handbook of ionogram interpretation and reduction*, Second edition, November 1972.

[4] Terkildsen, M., Neudegg, D., *Ionospheric research activities addressing space weather user requirements in the middle and low latitudes*, 40th COSPAR Scientific Assembly, Moscow, Russia, August 2014.

8 Equivalent Vertical Ionograms

Additional work was conducted to optimize a tool that, starting from automatic interpretation of oblique soundings, could output other parameters for the ionospheric region traversed by a ray path. This involved the conversion of all the 384 high quality ionograms analyzed into vertical ionograms, using Martyns theorem (Martyn, D. F., 1935). According to Martyns equivalent path theorem, if f_o and f_v
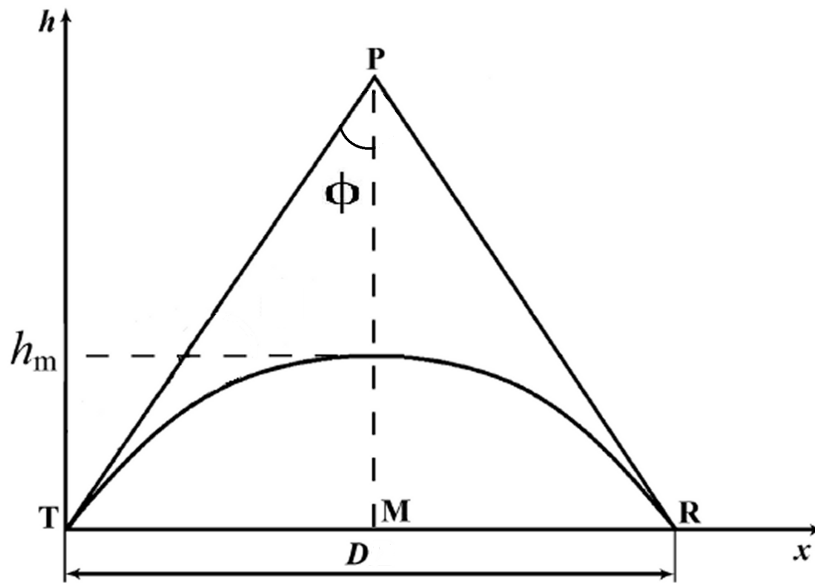
Figure 24: Martyns equivalent path theorem scheme: for radio transmission over a distance D the relationship between oblique and equivalent vertical frequencies is $f_o = f_v \sec(\Phi)$

are frequencies of radio waves reflected respectively obliquely and vertically from the same real height on a flat ionosphere (Gething, P. J. D., 1969), the virtual height of reflection of f_v, as schematically shown in Figure 24, is equal to the height of the equivalent triangular path for the signal:

$$\overline{TP} + \overline{PR} = 2\overline{PM} \sec(\Phi). \tag{31}$$

This theorem expresses an important relationship: the virtual height of reflection of an obliquely incident radio wave is the same as that of the equivalent vertical wave (Koltsov, V. V., 1969). This follows from the relationship between the refractive

indexes μ_o and μ_v for the oblique angle Φ and vertical waves at the same real height.

$$\mu_o \cos(\Phi) = \mu_v \cos(\Phi) \tag{32}$$

So, for a radio transmission over a distance D, the relationship between oblique and equivalent vertical frequencies is given by:

$$f_o = f_v \sec(\Phi). \tag{33}$$

New IDL code was developed to calculate the relative equivalent vertical ionogram for the CUR-MTE radio link including correction for the curvature of the Earth. Applying Martyns theorem to each frequency of the oblique sounding gives an equivalent vertical ionogram as shown in Figure 25. The procedure was applied to all the 384 IPS high quality oblique ionograms in order to better define the ionospheric characteristic along the path. Once the equivalent vertical ionogram had been defined it was recorded in an RDF file, a special file format for analysis by the Autoscala computer program, the INGV software for automatic interpretation of vertical ionograms. This technique enables modeling of all the ionospheric parameters of the vertical ionosphere in the region over a virtual ionosonde located at the mid point of the ray path. This kind of analysis will be important for the future development of a computer program that will combine parameters derived from both oblique and equivalent vertical ionograms to provide useful information on the structure of the ionosphere along a ray path.
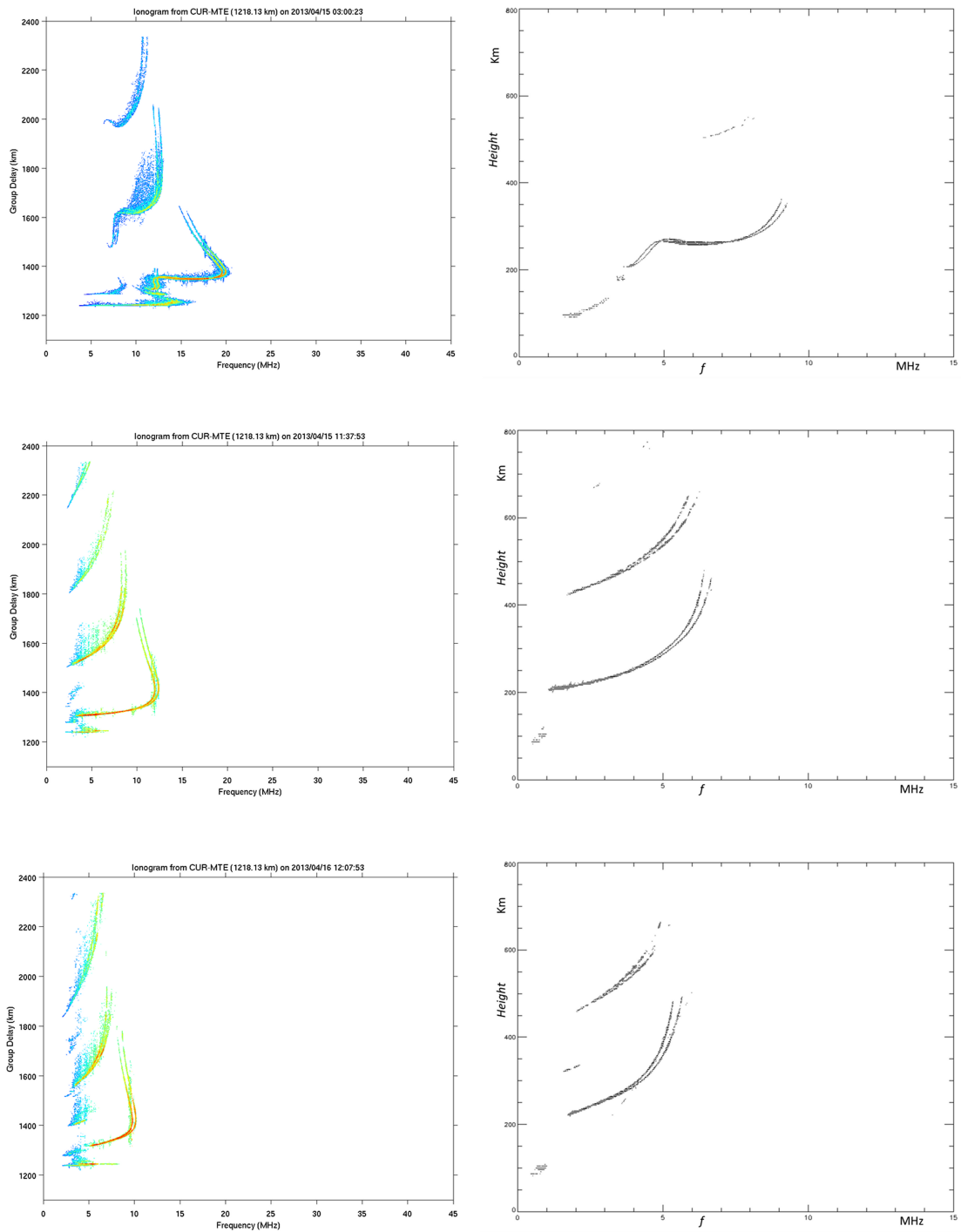
Figure 25: Examples of vertical ionograms obtained from oblique ionograms using Martyn's theorem. The oblique soundings were recorded on the CUR-MTE radio link respectively on 15 April 2013 at 03:00 , 15 April 2013 at 11:37 and 16 April 2013 at 12:07.

References

[1] Gething, P. J. D., *The calculation of electron density profiles from oblique ionograms*, Journal of Atmospheric and Terrestria Physics, vol. 31, pp. 347-35, 1969.

[2] Kol'tsov, V. V., *Determination of virtual reflection heights from oblique sounding data*, Geomagn. Aeron.(USSR), 9(5), 698-701, 1969.

[3] Martyn, D. F., *The propagation of medium radio waves in the ionosphere*, Proc. Phys. Soc., 47, 323-339, 1935.

9   Conclusions

The study and interpretation of oblique ionospheric soundings are important for constant monitoring of the Earth's ionosphere. Automatic scaling of oblique iono-grams offers a very useful way to analyze larger data sets in order to model the ionospheric layer. While a number of computer programs for automatic interpre-tation of vertical ionograms already exist, as yet there is no method for automatic scaling of ionospheric oblique soundings. In this work an algorithm for automatic scaling of oblique ionograms is presented for the definition of the Maximum Usable Frequency MUF for a given radio link. In developing the algorithm three crucial issues were addressed: the accuracy of the software in recognizing the MUF value from the ionogram; the rejection capabilities of the program to discard ionograms lacking sufficient information; the reliability of autoscaling in different geomagnetic conditions.

The autoscaling algorithm was applied to a large data set of INGV and IPS oblique ionograms producing good results in terms of accuracy. Among the results achieved it is notable that the software gives MUF values within a range of ± 1.5 MHz from the values provided by an expert operator for 100% of the ionograms with well de-fined traces, representing almost all the ionograms manually scaled by the operator. The rejection of low quality ionograms constitutes a major problem in space weather applications and the maximum contrast method also provides a criterion for discard-ing ionograms that do not have sufficient information, achieving a very high success rate as reported in the tables above. Only when C_{max} is higher than a fixed threshold C_t, the resulting curves are considered representative of the traces due to reflection from the F_2 region. Otherwise, the ionogram is deemed to lack sufficient information and is discarded with no MUF value provided as output. This avoids the occurrence of false positive events which would generate incorrect information on the structure of the ionosphere between the transmitter and receiver. The results show how the percentage of false positive events falls to 3.9% as the quality of the oblique sound-ings increases. It is also important to note that the algorithm does not discard ionograms in which an operator would consider the traces to be well defined.

The software was studied under different geomagnetic conditions, testing the algo-rithm on the same ionogram data sets, considering the different geomagnetic K_p indexes associated with each oblique ionogram analyzed. This proved that the pro-gram performance is not influenced by changing K_p values and the autoscaling algorithm performs well even under different geomagnetic conditions. It is worth noting that the analysis of the ionogram and autoscaling operations take less than two minutes for each oblique sounding, which is a very reasonable computational time for using the software as a now-casting procedure to detect certain important ionospheric characteristics.

In addition to automatic scaling of oblique ionograms, a ray tracing code was also developed to reconstruct the electron density profile along the ray path in question. The free parameters of the analytical model of the ionosphere are automatically changed until the synthetic oblique ionogram produced by the ray tracing program, matches the measured autoscaled ionogram. The ionospheric model which characterises the matched synthetic oblique sounding is then considered to be representative of the ionospheric region between transmitter and receiver.

An additional study was conducted on a high quality ionogram data set and a new algorithm was designed for the conversion of an oblique ionogram into a vertical ionogram, using Martyns theorem. This enables further analysis of data from oblique soundings using the INGV Autoscala program for automatic scaling of vertical ionograms.

The contents of this work have been described in the following scientific papers:

A. Ippolito, C. Scotto, M. Francis, A. Settimi, C. Cesaroni, *Automatic interpretation of oblique ionograms*, Advances in Space Research, in press.

A. Settimi, A. Ippolito, C. Cesaroni, C. Scotto, *Scientific review on the ionospheric absorption and research perspectives of a Complex Eikonal model for one-layer Ionosphere*, International Journal of Geophysics, vol. 2014, 2014.

C. Cesaroni, C. Scotto, A. Ippolito, *An automatic quality factor for Autoscala foF2 values*, Advances in Space Research, Volume 51, Issue 12, 15 June 2013, Pages 2316-2321, ISSN 0273-1177.

And have been presented at the following international conferences:

A. Ippolito, C. Scotto, D. Sabbagh, V. Sgrigna, *A procedure for the automatic scaling of oblique ionograms*, URSI AT-RASC 2015, Gran Canaria, Canary Islands May 18 -22 2015.

A. Ippolito, M. Francis, M. Layoun, M. Parkinson, D. Neudegg,*IPS oblique ionograms automatic scaling*, 14th Australian Space Research Conference (ASRC), Adelaide (Australia), 29 September October 1, 2014.

A. Ippolito, C. Scotto, C. Cesaroni, *Oblique ionograms automatic scaling and eikonal based ray tracing*, European Geosciences Union General Assembly 2013, WIEN 07 12 April 2013.

C. Cesaroni , A. Ippolito, C. Scotto, L. Ciraolo, *Topside-plasmasphere electron density profiles model by using AIS ionosonde measurements and calibrates GPS TEC data*, European Geosciences Union General Assembly 2013, WIEN 07 12 April 2013.